


Accelerating discovery, enabling scientists
Discover the benefits of using spectral flow cytometry for high-parameter, high-throughput cell analysis



SONY
Download Tech Note



GATA-3 Dose-Dependent Checkpoints in Early T Cell Commitment

This information is current as of August 8, 2022.

Deirdre D. Scripture-Adams, Sagar S. Damle, Long Li, Koorosh J. Elihu, Shuyang Qin, Alexandra M. Arias, Robert R. Butler III, Ameya Champhekar, Jingli A. Zhang and Ellen V. Rothenberg

J Immunol 2014; 193:3470-3491; Prepublished online 29 August 2014;
doi: 10.4049/jimmunol.1301663
<http://www.jimmunol.org/content/193/7/3470>

Supplementary Material <http://www.jimmunol.org/content/suppl/2014/08/28/jimmunol.1301663.DCSupplemental>

References This article **cites 54 articles**, 27 of which you can access for free at:
<http://www.jimmunol.org/content/193/7/3470.full#ref-list-1>

Why *The JI*? Submit online.

- **Rapid Reviews! 30 days*** from submission to initial decision
- **No Triage!** Every submission reviewed by practicing scientists
- **Fast Publication!** 4 weeks from acceptance to publication

**average*

Subscription Information about subscribing to *The Journal of Immunology* is online at:
<http://jimmunol.org/subscription>

Permissions Submit copyright permission requests at:
<http://www.aai.org/About/Publications/JI/copyright.html>

Email Alerts Receive free email-alerts when new articles cite this article. Sign up at:
<http://jimmunol.org/alerts>

The Journal of Immunology is published twice each month by
The American Association of Immunologists, Inc.,
1451 Rockville Pike, Suite 650, Rockville, MD 20852
Copyright © 2014 by The American Association of
Immunologists, Inc. All rights reserved.
Print ISSN: 0022-1767 Online ISSN: 1550-6606.



GATA-3 Dose-Dependent Checkpoints in Early T Cell Commitment

Deirdre D. Scripture-Adams,¹ Sagar S. Damle,² Long Li,³ Koorosh J. Elihu,⁴ Shuyang Qin, Alexandra M. Arias, Robert R. Butler, III,⁵ Ameya Champhekar,⁶ Jingli A. Zhang,⁷ and Ellen V. Rothenberg

GATA-3 expression is crucial for T cell development and peaks during commitment to the T cell lineage, midway through the CD4⁺ CD8⁻ (double-negative [DN]) stages 1–3. We used RNA interference and conditional deletion to reduce GATA-3 protein acutely at specific points during T cell differentiation in vitro. Even moderate GATA-3 reduction killed DN1 cells, delayed progression to the DN2 stage, skewed DN2 gene regulation, and blocked appearance of the DN3 phenotype. Although a Bcl-2 transgene rescued DN1 survival and improved DN2 cell generation, it did not restore DN3 differentiation. Gene expression analyses (quantitative PCR, RNA sequencing) showed that GATA-3-deficient DN2 cells quickly upregulated genes, including *Spi1* (PU.1) and *Bcl11a*, and downregulated genes, including *Cpa3*, *Ets1*, *Zfp1*, *Bcl11b*, *Il9r*, and *Il17rb* with gene-specific kinetics and dose dependencies. These targets could mediate two distinct roles played by GATA-3 in lineage commitment, as revealed by removing wild-type or GATA-3-deficient early T lineage cells from environmental Notch signals. GATA-3 worked as a potent repressor of B cell potential even at low expression levels, so that only full deletion of GATA-3 enabled pro-T cells to reveal B cell potential. The ability of GATA-3 to block B cell development did not require T lineage commitment factor Bcl11b. In prethymic multipotent precursors, however, titration of GATA-3 activity using tamoxifen-inducible GATA-3 showed that GATA-3 inhibits B and myeloid developmental alternatives at different threshold doses. Furthermore, differential impacts of a GATA-3 obligate repressor construct imply that B and myeloid development are inhibited through distinct transcriptional mechanisms. Thus, the pattern of GATA-3 expression sequentially produces B lineage exclusion, T lineage progression, and myeloid-lineage exclusion for commitment. *The Journal of Immunology*, 2014, 193: 3470–3491.

Gata3 is required for T cell development, but the mechanisms by which it works are only partially understood. *Gata3* is expressed in a number of embryonic tissues as well as in the thymus, and the germline knockout generates an embryonic lethal phenotype before the earliest T development stages, between embryonic day (E)11 and E12 in *Gata3* knockout pups (1). Rag2^{-/-} blastocyst complementation experiments show that *Gata3*-null embryonic stem cells can contribute to all hematopoietic lineages except the T lineage (2–5). Experiments showing that antisense oligonucleotides to *Gata3* could block appearance of CD3⁺ cells in fetal thymic organ culture provided initial evidence that GATA-3 acts after thymic entry (6). GATA-3 is also required for generation of the earliest intrathymic precursors (7), and in

some conditions regulates self-renewal behavior of prethymic stem cells as well (8, 9). Poor viability of the earliest T cell precursors when GATA-3 is removed prethymically (7) has limited exploration of the role GATA-3 plays in T cell specification and commitment, and Lck-Cre deletes a conditional allele too late to probe a role in lineage commitment as such (10). However, recent work has linked GATA-3 to the important decision of T cell precursors to eliminate B cell potential in the double negative (DN) stages 1 and 2 (11). The present study was undertaken to introduce stage-specific, acute, early perturbations of GATA-3 that could shed light on its actions between thymic entry and commitment.

Ideally, the roles of GATA-2 could be inferred from its target genes. GATA-3 binding sites have been mapped across the genome

Division of Biology and Biological Engineering, California Institute of Technology, Pasadena, CA 91125

¹Current address: Division of Hematology–Oncology, Department of Medicine, University of California Los Angeles AIDS Institute, Los Angeles, CA.

²Current address: Department of Bioinformatics, Antisense Drug Discovery, Isis Pharmaceuticals, Carlsbad, CA.

³Current address: Department of Cell Biology and Department of Immunology, Tianjin Medical University, Tianjin, People's Republic of China.

⁴Current address: Department of Anesthesiology, Harbor–University of California Los Angeles Medical Center, Torrance, CA.

⁵Current address: Department of Biology, Illinois Institute of Technology, Chicago, IL.

⁶Current address: Department of Microbiology, Immunology, and Molecular Genetics, University of California Los Angeles, Los Angeles, CA.

⁷Current address: Genentech, Inc., South San Francisco, CA.

Received for publication June 24, 2013. Accepted for publication August 4, 2014.

This work was supported by National Institutes of Health Grants R01CA98925, RC2CA148278, R01CA90233, and R01AI95943, the Louis A. Garfinkle Memorial Laboratory Fund, the AI Sherman Foundation, and the Albert Billings Ruddock

Professorship (to E.V.R.). Initial support for D.D.S.-A. was also provided by the Elisabeth Ross Endowment at the California Institute of Technology and by National Institutes of Health Training Grant 5T32 HD07257.

The sequences presented in this article have been submitted to the Gene Expression Omnibus (<http://www.ncbi.nlm.nih.gov/geo/query/acc.cgi?acc=GSE59215>) under accession number GSE59215.

Address correspondence and reprint requests to Dr. Ellen V. Rothenberg, Division of Biology and Biological Engineering, California Institute of Technology, 1200 East California Boulevard, Pasadena, CA 91125. E-mail address: evroth@its.caltech.edu

The online version of this article contains supplemental material.

Abbreviations used in this article: B6, C57BL/6; DN, double-negative; DP, double-positive; E, embryonic day; ER, estrogen receptor; EYFP, enhanced yellow fluorescent protein; FL, fetal liver; FLDN, FL-derived double-negative; FLP, FL-derived precursor; Flt3L, Flt3 ligand; FT, fetal thymus; ILC2, innate lymphocyte type 2; Lin, lineage; LZ, LZRS retrovirus; NGFR, nerve growth factor receptor; 4OHT, 4-hydroxytamoxifen; qPCR, quantitative real-time reverse transcriptase-dependent PCR; RNA-seq, RNA sequencing; SCF, stem cell factor; shRNA, short hairpin RNA; siRNA, small interfering RNA; YFP, yellow fluorescent protein.

Copyright © 2014 by The American Association of Immunologists, Inc. 0022-1767/14/\$16.00

in CD4⁺CD8⁺ thymocytes and earlier CD4⁻CD8⁻ (DN) precursors (12, 13). However, the distribution of sites detected has turned out to be variable according to stage, implying that GATA-3 regulates different target genes at different points in development. Complementing GATA-3-deficient cells with retroviral GATA-3 is also challenging because GATA-3 overexpression is as toxic for early T cell precursors as loss of GATA-3 (14). In this study, therefore, we have retrovirally introduced short hairpin RNA (shRNA) into precursors undergoing T lineage differentiation *in vitro* (15, 16) to impose loss of function at specific precommitment, pro-T cell stages, and we have examined the effects of acute *Gata3* deletion at short time scales. We show that a critical level of GATA-3 activity is needed to progress through commitment, and demonstrate that GATA-3 contributes directly and uniquely to T lineage commitment through two different mechanisms.

Materials and Methods

Mice

C57BL/6 (B6), B6D2 F₂, or E μ -Bcl-2-25 (Bcl-2-tg) (17) mice were used. B6 or E μ -Bcl-2-25 (Bcl-2-tg) fetal mice were generated in our colony, and B6 \times DBA/2 (B6D2) F₂ embryos were obtained from the California Institute of Technology Genetically Engineered Mouse Service. ROSA26R-enhanced yellow fluorescent protein (EYFP) reporter mice for Cre-mediated excision (18) were bred from stock donated by Dr. Frank Costantini (Columbia University). *Gata-3*^{fl/fl} mice (10) were bred from stock provided by Dr. I-Cheng Ho. *Sp1*^{fl/fl} (PU.1 floxed) mice were provided by Dr. Stephen Nutt (19). *Bcl11b*^{fl/fl} (Bcl11b floxed) mice were previously described (20). ROSA26-Cre-ERT2 mice were generated in our colony by crossing PLBD (*Bcl11b*^{fl/fl}; ROSA26-Cre-ERT2) mice, provided by Dr. Pentao Liu (21), to B6 mice. To control the timing of *Gata3* deletion, these mice were further crossed to *Gata-3*^{fl/fl} mice to generate *Gata-3*^{fl/fl}; ROSA26-Cre-ERT2 mice. Note that unlike the ROSA26R-EYFP Cre recombinase reporter strains, these mice express Cre-ERT2 constitutively, but the nuclear localization and activity of the Cre protein depend on tamoxifen treatment. All animals were bred, maintained under specific pathogen-free conditions, genotyped, and euthanized using Institutional Animal Care and Use Committee-approved protocols.

Cell lines

Adh.2C2, the pro-T cell-line Adh.2C2 cell line, originally subcloned from the SCID.adh cell line (22), was generated and maintained as previously described (23). The murine macrophage-like cell line RAW264.7 was used as a negative control for specificity of GATA-3 intracellular staining. OP9 stromal cell lines, which either did (OP9-DL1, OP9-DL4) or did not (OP9-control) express Delta-like ligands, were obtained from J.C. Zúñiga-Pflücker and cultured as previously described (15, 16, 24).

Fetal liver-derived DN cells

E13.5–14 fetal liver (FL) was obtained from timed pregnancies of mice of the indicated genotypes. Differentiated cells were depleted using a mixture of biotinylated Abs specific for Ter119, Gr-1, F4/80, and CD19 (lineage [Lin] mixture) using tube adherence to a block magnet followed by a further depletion step on a MACS Miltenyi LS column (Miltenyi Biotec). They were then sorted for c-Kit⁺/CD27⁺/Lin⁻/7-aminoactinomycin D⁻ phenotype (Lin indicates depletion mixture above). These cells are referred to as FL-derived precursors (FLPs). To generate FL-derived DN (FLDN) cells, sorted precursors (15–100 \times 10³/plate) were added to 10-cm confluent plates of OP9-DL1 or OP9-control stroma and cultured for 6–7 d (OP9-DL1 condition). Cells were recovered from these cultures and infected overnight with retroviral vectors (performed as previously described) (25). From these transduced pools, ETP, DN2, and DN3 FLDN cells were sorted based on expression of GFP, c-Kit, CD25, and CD44, with CD45 to exclude stromal cells, prior to subsequent culture. For comparison, *in vivo* ETP, DN2, DN3, and DN4 cells were sorted from E14.5 fetal thymus (FT) or from the thymus of 4- to 6-wk-old adult mice after magnetic bead depletion with Lin mixture supplemented with Abs against TCR β , TCR $\gamma\delta$, CD8, NK1.1, and CD11b (Mac1), or using Abs against CD3, CD4, CD8, CD19, and Ter119 for experiments shown in Fig. 1F and Supplemental Fig. 1.

Flow cytometry

Flow cytometric analysis was performed on a BD FACSCalibur (BD Biosciences, Mountain View, CA) or MACSQuant (Miltenyi Biotec); sorts were done using either BD FACSVantage SE or the BD FACSAria IIu.

CD45 was used in all cases to discriminate between infected developing hematopoietic cells and OP9-derived stromal cells. The following Ab conjugates (BD Pharmingen and eBioscience) were used: c-Kit-PE, CD27-allophycocyanin, Gr-1-biotin, Ter119-biotin, F4/80-biotin, and CD19-biotin for sorting FL precursors; c-Kit-PE, CD44-PE-Cy5.5, CD45-allophycocyanin, CD25-Alexa Fluor 750 or CD25-allophycocyanin-Cy7, and streptavidin-Alexa Fluor 405 for sorting FT and FLDN precursors.

Four-color staining with intracellular GATA-3 and PU.1

Intracellular staining of transcription factors was performed using a modified version of the BD Cytofix/Cytoperm protocol. Abs used were BD Pharmingen clone L50-823 for GATA-3 and Cell Signaling Technology clone 9G7 for PU.1. Three-color surface staining was performed as normal. Cells were washed once to remove Ab and then pelleted and aspirated. Cells were then resuspended to disrupt the cell pellet prior to addition of 100 μ l cold BD Cytofix/Cytoperm and followed by a 20-min incubation on ice. Subsequently, 1 ml/tube \times PermWash was added and cells were pelleted and resuspended in 100 μ l \times PermWash/tube plus intracellular staining Ab. For both Gata-3 and PU.1, 20 μ l Ab per 1 million cells was used, and the equivalent microgram concentration was used for staining with isotype control Ab from the same supplier (BD Pharmingen or Cell Signaling Technology). The cells were incubated with intracellular staining Ab for 30 min at room temperature. Following this, 1 ml \times PermWash per tube was added to wash. Cells were then resuspended in 2% formaldehyde in PBS and data were acquired by flow cytometry within 1–2 d. Critically, for four-color staining that included staining for intracellular GATA-3 or PU.1, fully stained three-color plus intracellular isotype controls were used to determine accurate, population-specific background levels for GATA-3 and PU.1.

Retroviral vectors and infection of cells

The original Banshee retrovirus was provided by Dr. John Rossi (Beckman Institute of the City of Hope). Dr. Gabriela Hernandez-Hoyos constructed the Banshee-GATA-3 shRNA-expressing virus (called Banshee G3-3W), a derivative of a previously published GATA-3 shRNA construct (26) that incorporates two wobble mutations to prevent self-inactivation of the viral transcript (27) and a slightly altered loop sequence (TTCGTAGC rather than TAGCTTCG) (27). The sequence targeted is in exon 2, the first translated exon, immediately after the second in-frame Met codon. Controls were empty Banshee vector or Banshee driving expression of a scrambled shRNA insert.

LZRS retrovirus (Lz)-based construct Lz-GATA-3 was previously described (26, 28). Other constructs were made by members of the Rothenberg laboratory as follows. Lz-G3-ENG and a related GATA-2 construct, Lz-G2-ENG, were constructed (by Sanket Acharya and Mark Zarnegar) using fusion/overlap PCR to join the first 298 aa of *Drosophila* engrailed protein to the DNA binding domains of GATA-2 (aa 250–437) and GATA-3 (aa 251–443) to yield products with intact engrailed N termini and intact GATA factor C termini. PCR products were cloned into pGEM-T Easy, transferred to pEF1-Myc-His A to screen for orientation, and then excised by EcoRI/XhoI digestion and cloned into Lz. Lz(estrogen receptor [ER]) was constructed by Elizabeth-Sharon David-Fung by cloning the tamoxifen-dependent ER from STAT6-ER (provided by Naoko Arai, DNAX) (29) into Lz. Lz-GATA-3(ER) was then constructed by cloning full-length GATA-3 into Lz(ER), retaining the 5-aa linker SNSDP between the GATA-3 C terminus and the ER sequence. Lz-CRE-nerve growth factor receptor (NGFR) was constructed by Dr. Tom Taghon (Ghent University, Ghent, Belgium). Bcl-xL cDNA cloned into the MigR1 vector was purchased from Addgene (Cambridge, MA).

Retroviral infections of FLP in most experiments were carried out overnight with virus bound to plates coated with 50 μ g/ml RetroNectin (TaKaRa Bio, Tokyo, Japan). Conditions were essentially as previously described (25), except that unbound virus was not removed from the RetroNectin-coated wells prior to addition of cells and fresh media. Infections of fetal thymocytes and cells beginning T cell development by coculture with OP9-DL cells were carried out as described for individual experimental protocols.

Nucleofection

Direct nucleofection of Lin-depleted FL precursors was done using the Amaxa nucleofection system (Lonza) with a T cell kit and the X-001 program. Control small interfering RNA (siRNA; RISC-free, Dharmacon RNAi Technologies/Thermo Scientific) was transfected in parallel with a Gata-3-targeted siRNA (Dharmacon). Amaxa's pMAX GFP construct was transfected simultaneously to monitor transfection efficiency in some experiments. After transfection, cells were recovered and transferred to OP9-DL1 layers for recovery overnight, then sorted to purity using the same depletion protocol as described for derivation of FLDN cells. Adh.2C2 and RAW264.7 cells were transfected as described previously (23, 30).

Gene expression comparison of *FLDN* with DN subsets from primary FT and adult thymus

FLDN cells, obtained after 6 d of coculture with OP9-DL1, were sorted based on CD45, CD25, c-Kit, and CD44 for purification of total cell RNA, and equivalent DN populations were sorted by CD25, c-Kit, and CD44 expression from Lin-depleted FT (E14.5) and adult thymic DN cells in two independent biological replicates for each type of sample. cDNAs from these three types of DN1–4 populations were compared by quantitative real-time reverse transcriptase-dependent PCR (qPCR) for the genes shown in Fig. 1F and Supplemental Fig. 1, showing levels expressed relative to β -actin.

qPCR and primers

Primer sequences, RNA preparation methods, and qPCR conditions have been reported previously (14, 20, 25, 31). Additional primers are listed in Table I.

Single-cell cultures with *Gata3* shRNA

Retrovirus-transduced FL precursors were sorted at one cell per well directly into 96-well plates preseeded with OP9-DL1 or OP9 control cells. Wells were assessed for growth by microscopy and equal numbers of wells of *Gata3* shRNA-expressing and control-infected cells were harvested at 8 d and then stained for developmental markers. All remaining wells were harvested on day 12, and the additional identified expanding clones, although not included in Fig. 4A, were analyzed and included in the progression quantitation shown in Fig. 4B. Similarly, single infected ETP cells were directly sorted from wild-type or Bcl-2-transgenic mouse thymocytes into individual OP9-DL1 coculture wells and cultured either 7 (wild-type) or 9 d (Bcl-2 transgenic, not shown) prior to analysis. Descendants of singly plated cells were scored for developmental progression by tallying the stages through which each clone's descendants had passed (using a 10% frequency cutoff to determine what counts as progression). Thus, a clone in which 40% of cells are in DN1, 49% in DN2, 11% in DN3, and 0% in DN4 would be scored as having achieved progression to DN1, DN2, and DN3, but not DN4. Input cells were sorted initially as GFP⁺, but survival pressure on the cells frequently resulted in outgrowth of some GFP⁻ cells in the colonies. Although these were also usually inhibited in progression past DN2 when the G3 shRNA was present, developmental progression scoring (e.g., Fig. 4B) was based only on the cells remaining GFP⁺.

Switch cultures of DN2 cells from *Gata3*, *Bcl11b*, and *Bcl11b*; *Gata3* homozygously floxed mice

Cells were taken from mice with homozygously floxed alleles of the indicated genes or control +/+ genotypes, all crossed onto the ROSA26R-EYFP background. For experiments shown in Fig. 7, Cre retroviral infection of Ter119⁻, Gr-1⁻, and CD19-depleted FL precursors was carried out in the presence of 5 ng/ml each Flt3L ligand (Flt3L), IL-7, and stem cell factor (SCF; c-Kit ligand). The next day, Lin⁻c-Kit⁺CD27⁺YFP⁺ cells were sorted preparatively and stored in frozen aliquots at $5\text{--}6 \times 10^3$ cells/vial or used to seed cultures immediately. Thus, the controls as well as the conditional deletion samples were Cre treated and validated to have expressed active Cre. In these experiments, OP9-DL4 stroma were used to support T cell development. The cells were cultured on OP9-DL4 for an initial 7–9 d with 5 ng/ml each Flt3L, SCF, and IL-7 before preparative sorting of DN2 cells. SCF was added to the primary cultures in an attempt to preserve viability of GATA-3-deficient DN1 cells by providing stronger c-Kit signaling. Some apparent violation of the DN2 block in the primary cultures of Cre⁺ *Gata3*^{fl/fl} cells was occasionally seen in these experiments, but this was a result of the overpowering selection (Fig. 7B) for cells that had retained one undelated *Gata3*^{fl} allele during the ETP stage, and were thus heterozygotes, as revealed in Fig. 7G. Only sorted c-Kit⁺CD44⁺CD25⁺CD45⁺CD19⁻ DN2 cells from the primary cultures were transferred to secondary cultures, where 1% were moved to fresh OP9-DL4 cells and the rest were challenged by shifting to the OP9-control environment. Thus, any CD19⁺ cells that emerged later came from cells that had undergone at least a week of strong Notch signaling in culture and had then been sorted for a T lineage, CD19⁻ phenotype. For limiting cell-number cultures of DN2 cells from the FLDN primary cultures, 25 cells/well were deposited by cell sorting into microtiter wells preseeded with OP9-control cells, then cultured with 5 ng/ml each IL-7 and Flt3L. These cultures were harvested for analysis after 2 wk.

Switch cultures of adult bone marrow-derived DN2 cells from *Gata3*^{fl/fl}; ROSA26-Cre-ERT2 mice

Bone marrow stem cells from control ROSA26-Cre-ERT2 and *Gata3*^{fl/fl}; ROSA26-Cre-ERT2 mice were sorted as Lin⁻Sca-1⁺c-Kit⁺ (LSK) and

cultured on OP9-DL4 with 5 ng/ml Flt3L and IL-7 for 11 d. 4-Hydroxytamoxifen (4OHT) was added into the culture at 0.1 μ M for 16 h. DN2 cells were then sorted and shifted to OP9-control stromal cocultures with Flt3L and IL-7 at 5 ng/ml, but without tamoxifen, for 10 d before FACS analysis. For the colony assay experiment shown in Fig. 8G, the DN2 cells were sorted and cultured in retroviral infection conditions with Bcl-x_L or empty vector virus, in the presence of 4OHT to induce Cre activity. The cells were sorted again to purify GFP⁺ Bcl-x_L or empty vector virus-infected cells. The sorted cells were then transferred to 96-well plates at inputs of 25 cells/well for 2 wk with OP9-control stroma, Flt3L, and IL-7 to permit B cell development.

Acute homozygous and heterozygous *Gata3* deletion

To examine short-term impacts of deleting *Gata3*, *Gata3*^{fl/fl} or *Gata3*^{fl/+} embryos with a ROSA26R-EYFP homozygous or heterozygous genetic background were obtained at E13.5 as a source of FLP and started into T cell development by a 4-d preculture on OP9-DL1. They were then transduced with retroviral Cre for 4 h, returned to OP9-DL1 overnight (18 ± 2 h), and sorted the next day to purify YFP⁺ (successfully Cre-transduced) cells. These were then either analyzed immediately or returned to OP9-DL1 coculture. To analyze the effect of deleting a single copy of *Gata3*, YFP⁺ DN1 cells were sorted, returned to secondary culture for 7 d, and finally the DN2a, DN2b, and DN3 YFP⁺ cells generated were analyzed and/or sorted for RNA expression analysis, in comparison with control Cre-transduced YFP⁺ cells derived from ROSA26R-EYFP *Gata3*^{+/+} mice. Retroviral marker expression (NGFR) was highly concordant with activation of the ROSA26R-EYFP reporter gene by Cre-mediated excision of the stop cassette. To avoid confounding effects due to cell death, gene expression responses to deleting both copies of *Gata3* were analyzed only after shorter times. Cycloheximide chase experiments in 2C2 cells, analyzed by intracellular staining and Western blotting (S. Qin, G. Freedman, and S. S. Damle, data not shown), had verified that GATA-3 protein has a $t_{1/2}$ of only ~ 2 h. Therefore, after Cre transduction and overnight coculture with OP9-DL1, YFP⁺ DN1, YFP⁺ DN2a, and sometimes also YFP⁺ DN2b cells were sorted for immediate RNA analysis by qPCR (i.e., within <1 d of Cre introduction). To generate homozygously *Gata3*-deleted DN2 samples for whole-genome surveys using RNA sequencing (RNA-seq), a similar protocol was used.

Pooling of multiple datasets, statistics

Means shown for RNA expression and cell numbers are geometric means, and error bars represent 1 SD from the means. Statistical significance was calculated using a two-tailed *t* test, and $p < 0.05$ was considered significant. Alternatively, for sample sets with low *n* and non-normal distributions, the Mann–Whitney–Wilcoxon *U* test (two-tailed) was used to calculate *p*, using the Web site <http://elegans.som.vcu.edu/~leon/stats/utest.html>.

RNA-seq analysis

Two RNA-seq comparisons were done. In each, ROSA26R-EYFP⁺ *Gata3*^{fl/fl} cells were transduced with Cre retrovirus to generate putatively *Gata3*-deleted cells, identified as EYFP⁺ DN2 cells. One experiment compared Cre⁺ *Gata3*^{fl/fl} cells with Cre retrovirus–transfected B6 DN2 cells (*Gata3*^{+/+}, DN2 pool $\sim 50\%$ transduced), and the other compared Cre⁺ *Gata3*^{fl/fl} cells with control virus–transduced *Gata3*^{fl/fl} cells (same genetic background but without deletion). Libraries for RNA-seq analysis were generated by the Jacobs Genetics and Genomics Center at the California Institute of Technology essentially as described previously (13) with minor modifications, using NEBNext multiplex reagents (New England Biolabs) and determining single-end sequences on an Illumina HiSeq 2500 high-throughput sequencer. Raw sequence reads as fastq files were processed using TopHat (v2.0.6) to map to the mm9 mouse genome assembly, using Cufflinks (v2.1.1) to generate BAM files, bamToBed to generate BED files (BedTools v2.14.2), and then BedTools genomecov to generate bedgraph files that were normalized by the total number of mapped reads (RPM). For visualization in the University of California Santa Cruz genome browser (<http://genome.ucsc.edu>), we converted the bedgraphs to BigWig files. Data were deposited in Gene Expression Omnibus (accession no. GSE59215) (<http://www.ncbi.nlm.nih.gov/geo/query/acc.cgi?acc=GSE59215>).

Differential expression analysis was carried out as follows. First, results were filtered to remove small gene models (Snor, Mir, Rpl, and Rps) and genes with low expression values (less than five fragments per kb of exon per million fragments mapped [fpkm]). Then the remaining values (9580 gene models) were log₂ transformed (floor of 0.01), and a Pearson correlation matrix was computed for the four datasets. All four datasets cross-correlated with $r \geq 0.9$. The developmental staging of the samples was assessed by using an index set of 173 developmentally regulated genes

annotated as transcription regulators from our RNA expression data reported previously for wild-type FLDN cells and adult thymocytes (13). Values for these index genes in each experimental sample were compared with the values in our reference samples using principal component analysis. This analysis verified that the samples fall into the DN2a–DN2b interval as expected by differentiation time and surface phenotype. Then, two statistical approaches were applied to identify new candidates for particularly GATA-3-sensitive target genes. Cuffdiff (32) was used to identify differentially expressed genes in the two comparisons pooled together, and those with p values of <0.01 were considered significant. In parallel, genes with substantial differential expression within each pair were identified by rank product and reverse rank product in the two comparisons pooled together (downregulated and upregulated genes), with p values for the replicate comparisons calculated based on minimizing rank product/rank sum ($p < 0.005$) (33). Additional differential expression criteria were used for transcription factor genes as described in the text. The early time point chosen and the dynamic developmental context meant that only strongly and rapidly affected genes could be detected above background. However, this survey of limited statistical power was designed as a search tool to identify new candidates for rapidly GATA-3-sensitive genes that could be tested for validation in additional experiments, that is, the GATA-3 knockdown or deletion tests assayed by qPCR in independent experiments as presented in the text.

Results

Expression pattern of GATA-3 in T development

Gata3 is expressed in multipotent prethymic precursors for T development ($\text{Lin}^- \text{c-Kit}^{\text{hi}} \text{Sca-1}^{\text{hi}} \text{CD27}^+$ FL or bone marrow cells) (34). However, much higher *Gata3* expression is seen even in the most immature cells within the thymus (35), with only a little further increase (~ 3 -fold) in *Gata3* RNA during T lineage commitment (11, 13, 28, 31, 36). However, GATA-3 protein levels can be regulated by posttranscriptional mechanisms as well (37–41). We therefore measured GATA-3 protein content by direct intracellular staining in each of the early DN stages (Fig. 1A; *top panels* show gating strategy).

In adult B6 mice, GATA-3 protein is initially low in the $\text{c-Kit}^{\text{hi}} \text{CD44}^+ \text{CD25}^-$ (early T cell precursor) population, the subset of $\text{CD44}^+ \text{CD25}^-$ DN1 thymocytes that includes T cell precursor activity. GATA-3 levels barely change as the cells initiate expression of CD25 (DN1 25^{lo}), but rise ≥ 3 -fold as they turn on CD25 to become DN2a ($\text{c-Kit}^{\text{hi}} \text{CD44}^+ \text{CD25}^+$) (Fig. 1A, *middle*). Dissecting the DN2 stage by c-Kit expression levels to separate uncommitted from committed cells (42), the DN2b (c-Kit lower) newly committed cells have the highest levels of GATA-3 protein and RNA (Fig. 1A). DN3 cells ($\text{c-Kit}^{\text{lo}} \text{CD44}^{\text{lo}} \text{CD25}^+$) before β -selection or $\gamma\delta$ -selection express slightly less, with the lowest expression in a distinct subset of DN3 cells with no detectable c-Kit expression (DN3 c-Kit^-). In cells beginning β -selection (DN3 CD25^{lo}) and through the DN4 stage ($\text{c-Kit}^{\text{lo}} \text{CD44}^{\text{lo}} \text{CD25}^{\text{lo}}$), GATA-3 protein levels rise again (Fig. 1A, *bottom*) but then subside as the cells reach $\text{CD4}^+ \text{CD8}^+$ (double-positive, DP) stage (26). RNA levels, similar to protein levels, rise slightly in the DN2 and DN3 stages (Fig. 1B). This pattern is seen also in both $\text{Rag2}^{-/-}$ adult thymocytes and normal B6 fetal thymocytes, confirming that the increase does not depend on TCR gene rearrangement (Fig. 1C). These results agree well with the expression reported for *Gata3* knock-in alleles (3, 7, 11).

GATA-3 follows a similar pattern during T cell differentiation in vitro when $\text{c-Kit}^+ \text{CD27}^+ \text{Lin}^-$ precursors from E13.5 FL are cultured on OP9-DL1 stroma to generate DN pro-T cells (Fig. 1D, 1E). As shown by detailed expression comparisons of >55 genes in Supplemental Fig. 1 (for primers, see Table I), FLDN subsets prepared in this way correspond closely to normal primary fetal thymocyte DN subsets. Where the gene expression patterns differ, as illustrated for 25 transcripts in Fig. 1F, gene expression patterns in FLDN subsets are intermediate between those of E14.5 fetal

thymocyte subsets and those of corresponding adult DN thymocyte subsets. Thus, small variations in program dynamics reflect the ontogeny of the precursors more than the conditions of differentiation. Similar to fresh fetal thymocytes, FLDN cells have slightly higher *Gata3* RNA expression (Fig. 1B, 1F) and a slightly accelerated GATA-3 protein increase relative to adult thymocytes, peaking at DN2a and DN2b, then subsiding slightly from DN2b to DN3 (Fig. 1C, D). In all three sources of developing T cells, the timing of peak GATA-3 expression at DN2 suggests a role between thymic entry or initiation of T cell development and commitment.

Reduction of GATA-3 inhibits viability and population expansion

To test the effect of acutely downregulating GATA-3, we used Banshee G3-3W (Fig. 2A), a bicistronic retroviral shRNA expression construct with a GFP marker designed to block translation from *Gata3* transcripts specifically (26, 27). The magnitude, speed, and stability of knockdown using this construct were assayed by intracellular GATA-3 staining in the DN3-like Adh.2C2 cell line (23), with Raw264 myeloid cells, which do not express GATA-3, used as a specificity control (Fig. 2B). Retroviral expression of *Gata3*-specific shRNA reduced GATA-3 protein to $\sim 50\%$ within 20 h, stabilizing at $\sim 45\%$ of control levels for at least 6 d (Fig. 2C, 2D). Similarly, FLDN cells cultured for 6 d after infection with *Gata3* shRNA had GATA-3 protein levels reduced to $\sim 50\%$ of control in cells with DN2 and DN3 phenotypes and reduced to isotype control background levels in cells retaining a DN1 phenotype (Fig. 2E). For more extensive confirmation of the effects of this shRNA on *Gata3* RNA and GATA-3 protein in the Adh.2C2 system, also see our recent report (43). *Gata3* shRNA thus consistently lowered GATA-3 protein levels, despite its generally mild effect on RNA levels.

Even this modest reduction in protein expression had pronounced functional consequences. Six days after infection, Banshee G3-3W-infected Adh.2C2 cells were profoundly inhibited in proliferation, viability, and the ability to sustain vector GFP expression as compared with cells infected with control virus, implying that cells with most severe GATA-3 loss were being eliminated (Fig. 2F, 2G, *top panels*). When FLPs were infected with G3-3W and cultured with OP9-DL1 stroma (T cell conditions), a steep, progressive loss of virus-transduced GFP⁺ cells was seen after 48 h (Fig. 2G, *middle*; note time scale; also see Supplemental Fig. 2D). However, when the same precursors were cultured on OP9-control to promote B and myeloid development, the percentage of GFP⁺ cells continued to increase (Fig. 2G, *lower*; see Supplemental Fig. 2D). Thus, the effects of *Gata3*-specific shRNA expression faithfully reflect the T lineage-specific requirement for GATA-3.

The strength of these effects was surprising because no evident phenotype had been reported after Cre treatment of a simple *Gata3*^{fl/+} heterozygote. We also failed to detect substantial alterations in FLDN cell development in vitro from *Gata3*^{fl/+}; *ROSA26R-EYFP* cells that were transduced with Cre retrovirus and sorted for Cre-induced EYFP expression (Supplemental Fig. 2A). The normal cell surface phenotypes of these *Gata3* heterozygous cells were validated by their normal expression of a panel of developmentally regulated genes in the cells (Supplemental Fig. 2B). It was not possible to use GATA-3 intracellular staining to measure protein loss from the deleted allele because the targeted exons do not affect expression of the epitope detected. However, single-copy deletion of *Gata3* also consistently showed 60–80% of normal levels of *Gata3* RNA including the floxed exons, implying some compensation mechanism (Supplemental Fig. 2C

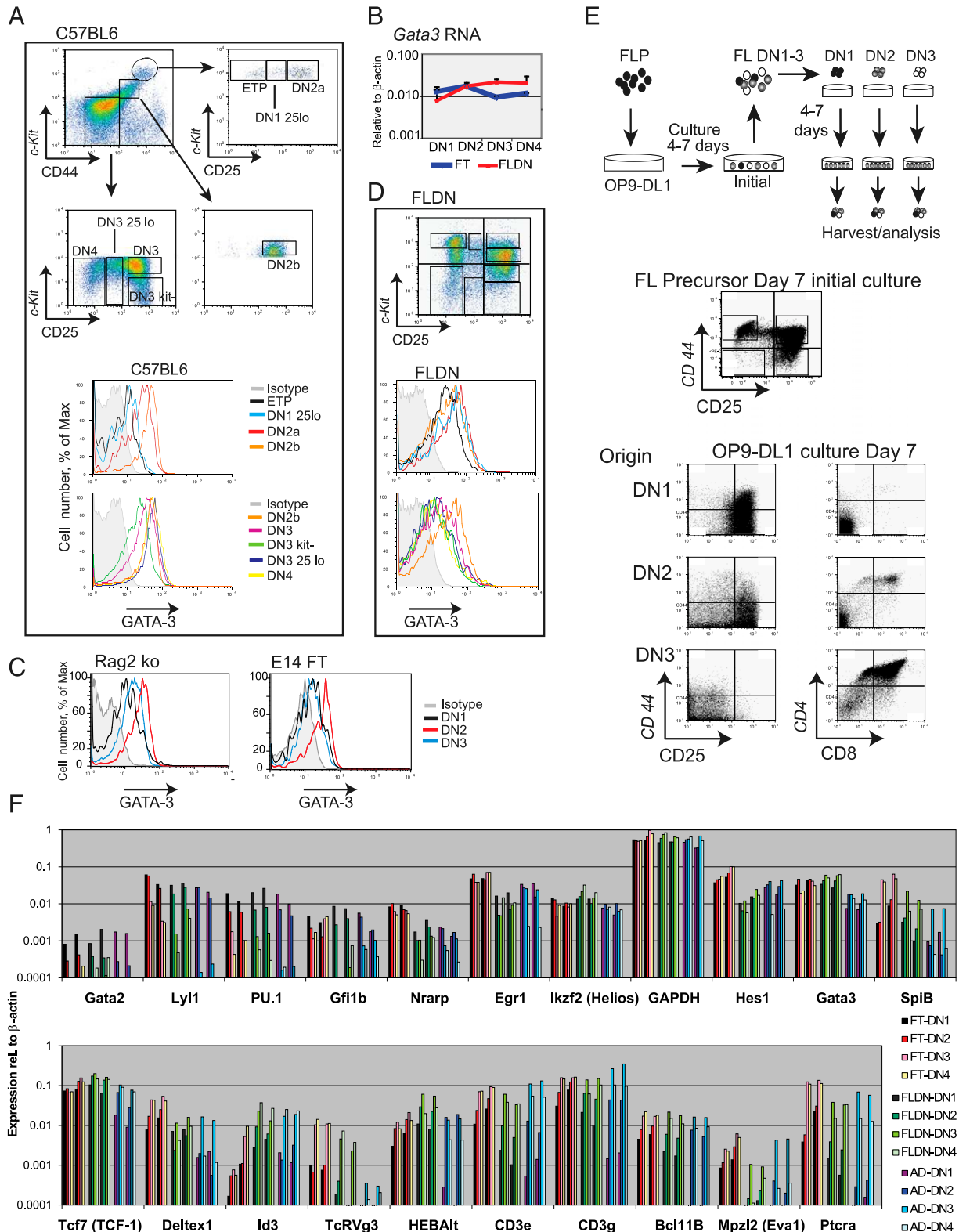


FIGURE 1. Expression patterns of GATA-3 in early T lineage cells. **(A)** Four-color intracellular detection of GATA-3 in early DN thymocyte subsets from B6 adult mice. *Top panels*, Subsets defined by expression of c-Kit, CD44, and CD25. *Lower panels*, Histograms showing GATA-3 protein levels. *Upper histogram*, Levels in stages from ETP to DN2b. *Lower histogram*, Levels in stages from DN2b to DN4 (DN2b is included in both for orientation). **(B)** *Gata3* RNA expression in DN1–DN4 cells. *Gata3* RNA levels were determined by qPCR analysis of samples from fetal thymocytes (FT) and FLDN cells generated as shown in **(E)**. *Gata3* expression levels are shown relative to β -actin for each sample. Results are from two (FT) or four (FLDN) independently sorted sample sets of DN1–DN4. **(C)** Intracellular staining of GATA-3 protein in cells from Rag-2^{-/-} weanling thymocytes and wild-type E14 fetal thymocytes. **(D)** Intracellular flow cytometric detection of GATA-3 protein in FLDN subsets derived as in **(E)** and gated as indicated (*top*). Histogram color coding is as in **(A)**. **(E)** Schematic of FLDN cell generation: FL precursors in OP9-DL1 coculture for 4–7 d (*top*) differentiate to DN1–DN3 stage pro-T cells (*middle*, day 7 initial culture). These are then sorted as pure subsets of DN1, DN2, and DN3 and replated on OP9-DL1 for 4–7 d more. Phenotypes shown are descended from the indicated sorted subsets after 7 more days of coculture (*lower panels*). **(F)** Gene expression (*Figure legend continues*)

Table I. New primers for qPCR: RNA expression analysis and genotyping

Gene	Forward Primer (5' → 3')	Reverse Primer (5' → 3')
RNA analysis		
Bcl11a	GTCTGCACACGGAGCTCTAA	CACTGGTGAATGGCTGTTTG
Bcl11b exons 2–4 ^a	AGGTCACCCCTGATGAAGAT	CATGTGTGTCTCTGCGGTGCT
Bcl11b exon 4 ^a	GGACAGCAATCCTTTCAACC	ATGACTCGGTCAAGGCACT
CD44	GCAGATCGATTTGAATGTAACC	GTCGGGAGATACTGTAGC
Spi1 (PU.1) alternate	CTCAGTCACCAGGTTTCC	TCCAAGCCATCAGCTTCTC
Thy1	GGGCGACTACTTTTGTGAGC	AGGGCTCCTGTTTCTCCTTG
TCRbC2	GGGTTCTGTCTGCAACCATC	CTATGGCCAGGGTGAAGAAC
TCRg cluster1	GCTGTGAGCACTGTGATAGCTC	TCAGCAACAGAAGGAAGGAAA
TCR V γ 3(5)-C γ 1	ATCGGATGAAGCCACGTACT	GAAGGAAAATAGTGGCTTGG
TCR V γ 2(4)-C γ 1	CGAAGCTATCTACTACTGTTCC	GAAGGAAAATAGTGGGCTTGG
TCRd	TACGACTGCTGTTTGCCAAG	TCTGAAGCACTGAGAAGTTGGA
Tcf7 (TCF-1)	CGAAGAGAGCAGGCCAAGTA	CCGAATGCATTTCTTTTCC
Tcf7 alternate	TCCCCATGCCAATACTTCTT	GTTGGTGCCAAGGTTGAAAG
Zfpml1 (FOG1) alternate	CCAAGATGTCGAGTTGGTG	GCGCTTGTGCACATAGAAGT
EBF-1	CCATCCGAGTTCAGACACCT	ATGCCGAGGAATGACCTTCT
Pax5 E2/E3	GAACCTTGCCCATCAAGGTTG	GAGTGGCAACCTTTGGTTTG
Pax5 E5/E6	GGGCTCCTCATACTCCATCA	CTGCTGCTGTGTGAACAGGT
Genotyping		
GATA-3 floxed	GGCATTCTCGCAGCTTCAAA (G3-F)	GGGCCGGTTCTGCCCAT (G3-R1)
GATA-3 deleted	GGCATTCTCGCAGCTTCAAA (G3-F)	GGATGGGCACCACCCCGTGAA (G3-R2)
Bcl11b deleted	ACGCCGGACCTAGTAAATGCA (B-F)	GTTAGGCTGGACTGCCGCCTC (B-R)

Primers described as “alternate” are new primers (used in Fig. 5B) for genes that we have measured in other experiments using other previously reported primers.

^aSame as described in Li et al. (20).

and the RNA-seq data presented later). Thus, the shRNA reduces GATA-3 expression more than the heterozygous deletion.

Reduced GATA-3 levels impair the DN2/DN3 transition

Reduced GATA-3 protein levels caused a stage-specific developmental block as well as reduced proliferation, as shown for sorted populations of Banshee G3-3W–transduced GFP⁺ FL precursors after 3–4 d of differentiation on OP9-DL1 (Fig. 3A, 3B, *left panels*). Direct nucleofection of a commercial anti-GATA-3 siRNA into such precursors gave similar results (Fig. 3A, *right panels*, siRNA). In both cases, the control cells were transitioning to DN3 stage at harvest, but the GATA-3 knockdown samples were blocked with a DN2 phenotype (Fig. 3A). A similar phenotype using this shRNA was also recently seen by Kee and colleagues (44).

The observed block was consistent with two possibilities. First, GATA-3 might need to act during DN2 stage to drive progression to DN3. Second, because of earlier roles of GATA-3 (7), the knockdown cells might simply be delayed in development. To distinguish between these possibilities, we allowed FL-derived precursors to develop normally to DN1, DN2, and DN3 stages in vitro, and only then transduced them overnight with control or *Gata3* shRNA–expressing retrovirus. Each infected subset was then sorted and returned to culture for further differentiation (Fig. 3C). FL-derived DN1 cells transduced with *Gata3* shRNA halted at DN2 stage in OP9-DL1 culture (Fig. 3C, FLDN1), and catastrophic failure of cell expansion accompanied this block (Fig. 3B, *right*). Even after cells had already developed to the DN2 stage, GATA-3 reduction delayed progression to DN3 (Fig. 3C, FLDN2) and often blocked it altogether (three of six experiments, not shown), implying that the DN2–DN3 transi-

tion was specifically vulnerable to loss of GATA-3. Notably, although decreased GATA-3 substantially inhibited FLDN1 and FLDN3 population expansion, the FLDN2 population was more resistant (Fig. 3B).

Loss of GATA-3 from FL-derived DN3 cells caused a delay in progression to the DP stage as well as severe loss of cellularity, as reported for conditional *Gata3* knockouts with Lck-Cre in vivo (10) (Fig. 3C, FLDN3). However, surviving cells from some of these GATA-3 knockdown samples displayed a “retrograde” CD44⁺ DN2-like phenotype (50% of DN3 knockdown experiments, data not shown). Thus, at a minimum, survival in the DN3 stage appears less tolerant of reduced levels of GATA-3 than in the DN2 stage.

E14–14.5 fetal thymocytes develop more rapidly than do FLDN cells in OP9-DL1 culture and pass more efficiently through DN2 to DN3 (Fig. 3D, 3E). By day 6.5, ~50% of control vector–transduced fetal thymocytes had acquired CD4 and/or CD8. However, when transduced with G3-3W, the great majority of fetal thymic DN1/ETP cells were blocked at DN2 at both early (3.5 d; Fig. 3D, *top*) and late (6.5 d; Fig. 3E, *top*) time points. Thus, the DN2 block is robust under both fast and slow development kinetics.

The DN2 stage block caused by GATA-3 knockdown is separable from growth inhibition

Severe cell loss raised the possibility that the DN2–DN3 developmental block might simply reflect apoptosis at DN3. To test whether viable cells are developmentally blocked, we knocked down expression of GATA-3 in Bcl-2–transgenic fetal thymic ETP cells. Bcl-2–transgenic E14–14.5 ETP cells survived ~3-fold better than did wild-type cells after knockdown of GATA-3, yet these cells went on to be severely DN2 arrested as did

comparison of sorted thymic T cell precursors with in vitro–generated FLDN subsets. Early DN thymocyte subsets from adult and fetal murine thymus were depleted of mature T and non-T lineage markers by magnetic bead binding and column selection and sorted into DN1–DN4 subsets. Two independent biological samples of each series were generated for this analysis. Adult thymus (AT) samples were composed of two adult mouse thymi per sorted biological sample. FT was obtained from E14/E14.5 fetuses from timed mated B6 mice. FLDN cells were OP9-DL1 cultured cells generated from c-Kit⁺Lin[−]CD27⁺E13.5/E14 FL precursors cultured on OP9-DL1 for 6 d, then sorted as shown into pure DN1, DN2, DN3, and DN4 developmental populations for analysis. Red/pink bars indicate the two sets of fetal thymic DN1–DN4; green bars, FLDN1–FLDN4; and blue bars indicate adult thymic DN1–DN4.

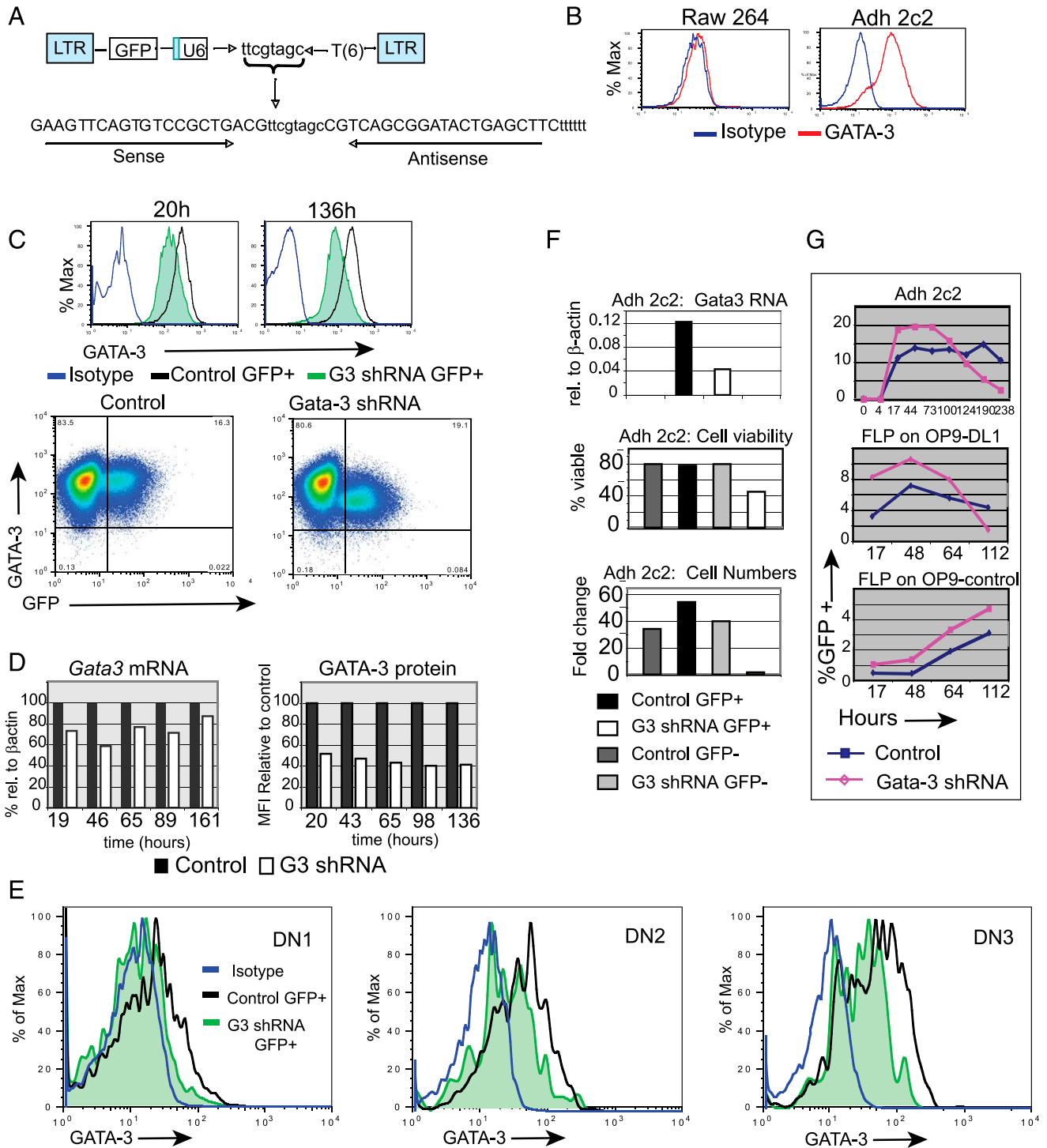


FIGURE 2. Specificity and efficiency of GATA-3 knockdown. **(A)** Map of G3-3W cloned in Banshee, showing *Gata3*-targeting shRNA sequences. **(B)** Specificity of intracellular flow cytometric staining in Adh.2C2 pro-T cells in comparison with RAW264.7 myeloid cells (negative control). For additional independent experiments on Adh.2C2 cells, see Del Real and Rothenberg (43). **(C)** Stable GATA-3 knockdown in Adh.2C2 cells after infection with G3-3W or control vector at 20 and 136 h (upper panels). Lower panels, Correlation of GFP reporter with GATA-3 knockdown. Intracellular GATA-3 staining of Adh.2C2 cells at 65 h postinfection with G3-3W or control vector is shown (also see Ref. 43). **(D)** Time courses of shRNA effects on *Gata3* RNA levels (left graph, qPCR) and GATA-3 protein levels in Adh.2C2 cells (right graph, intracellular staining). Values from GFP⁺ G3-3W transduced cells compared with GFP⁺ empty vector controls at the same time points are shown. RNA levels are normalized based on β -actin. For another independent experiment, see **(F)** (representative of at least three experiments); similar results for primary cells are shown in Fig. 5C, 5D. **(E)** Subset-specific effects of G3-3W shRNA on GATA-3 protein in FLDN cells. FLDN1, DN2, and DN3 subsets from OP9-DL1 culture were infected with G3-3W or control vector, then returned to culture, and intracellular flow cytometric staining was used to measure GATA-3 at 6 d after transduction. **(F)** Effects of GATA-3 knockdown on Adh.2C2 cells after 6 d. *Top*, Gata3 RNA levels in GFP⁺ cells. *Middle*, Viabilities, measured by 7-aminoactinomycin D exclusion, of GFP⁺ and GFP⁻ fractions of G3-3W-infected or control-infected cells. *Bottom*, Fold changes in cell numbers (same cell populations used in viability analysis; value of 1 indicates no change). Results of one experiment with Adh.2C2 cells are shown. **(G)** Comparison of GATA-3 knockdown effects on cell recovery in T lineage and non-T lineage cells. Maintenance of GFP⁺ populations (as percentage of total) after transduction with G3-3W (Gata-3 shRNA) or control constructs is shown for Adh.2C2 cells tracked during 238 h of culture (*top*), in primary E13.5 FLPs cultured for up to 112 h in T cell conditions on OP9-DL1 (*Figure legend continues*)

their nontransgenic counterparts (Fig. 3D, *lower panels*, and data not shown). Even when the Bcl2–transgenic fetal thymic ETP cells were cultured 6.5 d, *Gata3* shRNA–expressing ETP cells remained blocked at DN2, whereas control cells reached the DP stage (Fig. 3E, *lower*). Thus, the loss of the viability-promoting role of GATA-3 is not the sole cause for the observed arrest at DN2.

Clonal analysis of differentiation from single-cell precursors provided additional evidence that reduced GATA-3 could inhibit developmental progression separately from its role in survival and proliferation. Individual FL precursors infected with a control vector, sorted as GFP⁺ onto OP9-DL1 layers in 96-well plates, generated a range of descendants spanning all the early stages of T development after 8–12 d (Fig. 4A, *top*). The clonal descendants of *Gata3* shRNA–expressing FL precursors, in contrast, again were unable to progress beyond DN2 (Fig. 4A, *lower*). We quantified developmental progression by assuming that cells pass through DN1, DN2, DN3, and DN4 in order, and scored individual clones as “positive” for every stage that had been passed through by at least 10% of the cells in the clone at the time of analysis (see *Materials and Methods*). Using this scale to score progression in each clone, the developmental distributions of the control and GATA-3 knockdown clones are shown (Fig. 4B, *left*). No significant progression beyond DN2 was seen in any clones that grew from *Gata3* shRNA–transduced FL precursors (only 1 of 17 had >1% DN3 cells). In contrast, >40% of empty vector–transduced clones had reached DN3 or beyond (Fig. 4A, *top*, 4B and data not shown). Importantly, the *Gata3* shRNA–expressing clones could not surmount the DN2 block even in the cases where individual precursors had generated cell numbers comparable to controls (Fig. 4B, *right*). DN2 arrest was also observed with sorted single fetal thymocyte ETP cells expressing *Gata3* shRNA (Fig. 4C, *left*), and these ETP clones showed reduced expansion, consistent with behavior in bulk cultures (Fig. 4C, *right* and data not shown). Thus, T cell precursors with reduced GATA-3 levels are intrinsically inhibited from developmental progression to DN3.

GATA-3 conditional knockout confirms a requirement for GATA-3 for DN2–DN3 transition

To exclude off-target shRNA responses (45) as the cause of the DN2–DN3 block, we also tested the early GATA-3 role by inducing conditional deletion of the gene in vitro, infecting *Gata3*^{fl/fl} FLPs (10) with a Cre-expressing retrovirus before initiating T cell differentiation. More severe effects were expected in cells with complete loss of *Gata3* than with shRNA-induced dosage reduction (7, 11), but the question was whether any cells that did reach DN2 would be able to proceed to DN3. To minimize the number of cells in which *Gata3* could escape deletion, we sorted all cells for Cre vector expression after initial culture period on OP9-control stroma, and only then was T development triggered by transfer to OP9-DL1. As positive controls for Cre activity, cells from *Gata3*^{+/+} ROSA26R-EYFP fetal mice were transduced in parallel (Fig. 4D). Cre treatment of cells with a floxed *Gata3* allele showed that as with shRNA, development was blocked at DN2 (Fig. 4E), whereas Cre-treated control precursors progressed to DN4. Thus, this deletion model also demonstrated that GATA-3 was needed for transit from DN2 to DN3.

GATA-3 reduction causes derangement of the DN2–DN3 transitional program

The DN2–DN3 transition is defined not only by downregulation of CD44 but also by downregulation of c-Kit and, intracellularly, the downregulation of PU.1. Despite the strong effect on DN2–DN3 progression seen by criterion of CD44 expression, the G3-3W shRNA–treated cells continued to downregulate c-Kit expression almost similar to controls, implying that CD44 and c-Kit regulation had become divergent (Fig. 5A). The *Gata3* shRNA–transduced cells also appeared to increase their CD25 levels as a consequence of increased average cell size (data not shown), unlike normally progressing pro-T cells, which shrink on entering DN3a stage. This implied a more substantial defect in regulation of the DN2–DN3 program as a whole when GATA-3 levels are reduced.

The discordant c-Kit and CD44 levels raised the question whether the cells are intrinsically more similar to c-Kit^{lo} DN2 cells or CD44^{hi} DN3 cells. To resolve this, we transduced Bcl2–transgenic FLPs with G3-3W or scrambled shRNA, cultured them for a week on OP9-DL1, and then sorted DN1, DN2a, and DN2b subsets of the transduced GFP⁺ cells based on their c-Kit levels. Despite the presumed G3-3W effect on the protein levels of GATA-3, little effect on *Gata3* RNA was seen. However, the G3-3W–transduced cells that had reached DN1, DN2a, and DN2b-like phenotypic categories exhibited pronounced and specific gene expression abnormalities. Their elevated *Spi1* (PU.1) and *Bcl11a* and reduced *Bcl11b* and *Ets1* transcripts, in comparison with scrambled shRNA–transduced controls, implied an early DN2 arrest state. However, at the same time they also showed experimentally variable, precocious expression of the Notch-dependent DN2b–DN3-specific *HEBalt* transcript (an alternative promoter isoform of *Tcf12*) and the DN3-specific *SpiB* transcript (Fig. 5B, 5C).

Gene expression tests at earlier time points confirmed changes in gene expression that were discordant with normal developmental patterns as well (Fig. 5C, 5D). At 60 (Fig. 5C) or 40 h (Fig. 5D) after transduction with GATA-3 shRNA, PU.1 (*Spi1*) expression was repeatedly found slightly elevated in GATA-3 knockdown cells as compared with controls. At these earlier time points as well, *SpiB* and often *HEBalt* were found to be upregulated. The large experiment shown in Fig. 5C was carried out to measure short-term effects of GATA-3 knockdown on cells that were in precisely defined developmental stages before shRNA treatment, with RNA analysis then performed on progeny populations re-sorted as DN1, DN2, or DN3 after 60 h of further culture. The three experiments summarized in Fig. 5D tested earlier responses to transduction with G3-3W in primary E15.5 fetal thymocytes from Bcl2-transgenic mice. A consistent finding among the panel of developmentally significant genes measured was that *Spi1* levels were elevated relative to controls as early as 2 d after transduction (Fig. 5B–D), whereas onset of *Bcl11b* expression from ETP/DN1 precursors to DN2 was also dampened, although not maintenance of *Bcl11b* once already activated in late DN2 stage (Fig. 5B, 5C).

HEBalt depends on Notch signaling and HEB/E2A (46), so that the *HEBalt* upregulation seen in several short-term experiments (Fig. 5C and data not shown) implies that these crucial T cell regulatory inputs persist despite GATA-3 reduction (11). The normal or increased expression of Notch target genes CD25 (*Il2ra*) (Fig. 5B), *HEBalt* (Fig. 5C, 5D), and *Dtx1* (Fig. 5D) in *Gata3*-deficient cells also implies that Notch signaling con-

(*middle*), and in FLPs cultured in non-T cell conditions on OP9-control stroma (*lower*). Inhibitory effects shown in (F) and (G) are also representative of results in primary FL-derived precursors growing in T cell conditions (seven experiments) and FLDN cells recultured (seven experiments), although the 2C2 results shown are from a single experiment.

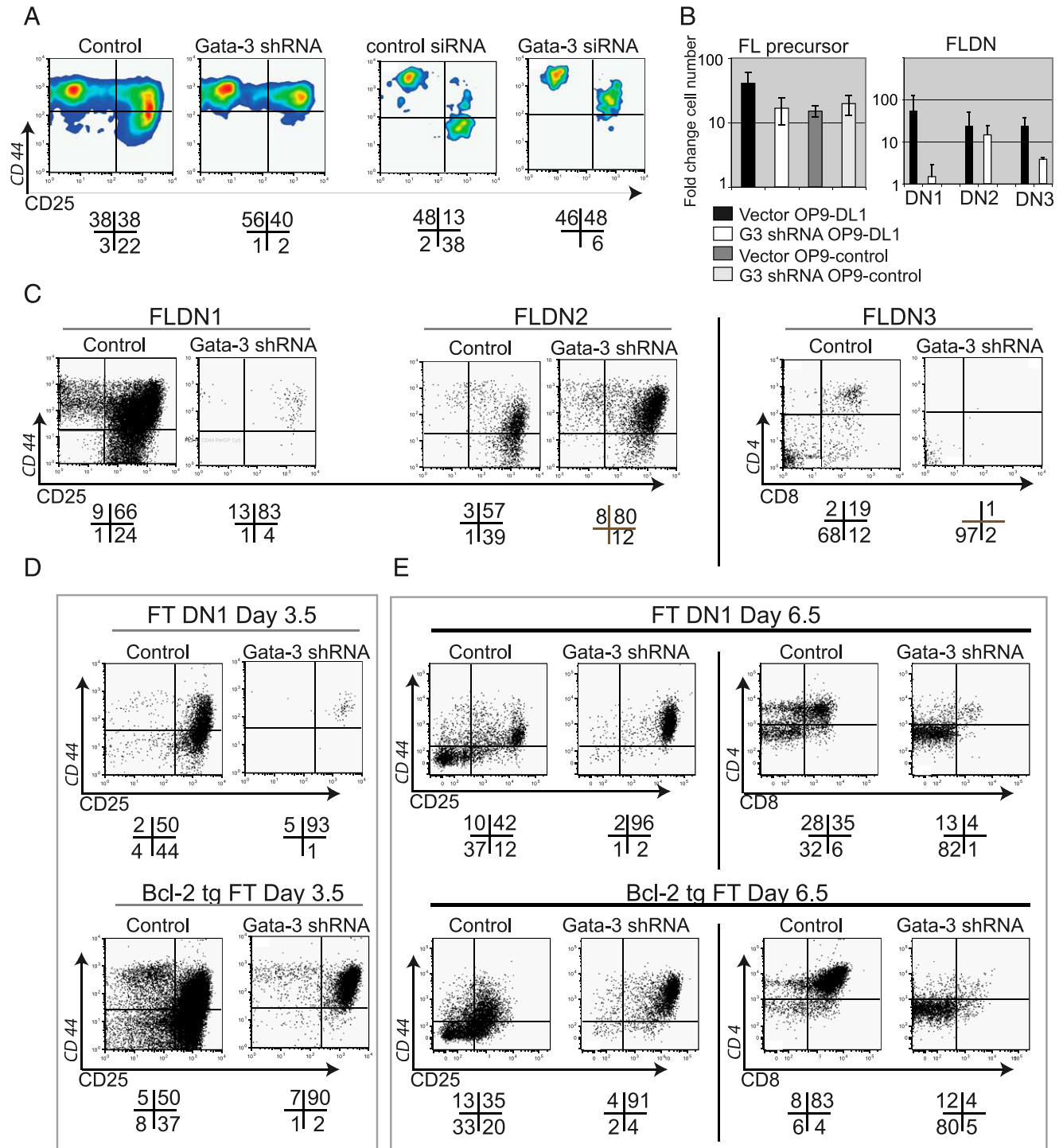


FIGURE 3. Developmental effects of GATA-3 knockdown. **(A)** Sorted FL precursors were transduced with G3-3W or control (*left panels*) or nucleofected with Gata-3-targeted or control siRNAs (*right panels*) and cultured on OP9-DL1 for 3.5 d. Numbers below plots show quadrant percentages. Data shown are representative of two retroviral infection and two nucleofection experiments. **(B)** Fold change in cell numbers for FL or FLDN subsets during a 3.5-d culture period is shown. *Left panel*, FL precursors treated as in (A) and cocultured with OP9-DL1 or OP9-control as in Fig. 2G. No significant differences in recovery were seen between G3-3W-transduced and control cells (two independent experiments). *Right panel*, Cell yields from FLDN cells generated as in Fig. 1E, then infected with control or G3-3W, sorted to pure vector-positive DN1, DN2, or DN3 subsets, then replated on OP9-DL1 for 5–7 more days. In three experiments, fold differences in yield of G3-3W versus controls were significant for FLDN1 ($p = 0.007$) and FLDN3 ($p = 0.007$). In three similar experiments with Bcl2-transgenic FLDN cells, G3-3W-transduced samples yielded only $20 \pm 3\%$ of the number of cells from control-transduced samples of FLDN1, DN2, and DN3 ($p = 0.004$, 0.006 , and 0.02 , respectively). **(C)** Developmental progression in FLDN subsets. FLDN cells were infected with control or G3-3W vectors, then sorted into purified subsets, returned to OP9-DL1 stroma for 5–7 d, and then analyzed. Numbers below plots are quadrant percentages. Data shown for DN2 precursors are representative of three experiments in which some breakthrough was seen, albeit in DN2 only; in three experiments there was no breakthrough. **(D)** Bcl-2-transgenic fetal thymic E14–14.5 ETP (Bcl-2 tg FT) and nontransgenic ETP (FT DN1) cells were sorted after infection with G3-3W or empty vector and cultured on OP9-DL1 for 3.5 d (representative of two experiments in which Bcl-2-transgenic and nontransgenic cells were cultured in parallel). Bcl-2 consistently enhanced yields but not progression. **(E)** A separate experiment from (D), but in this case cells were cultured 6.5 d on OP9-DL1 (representative of two experiments).

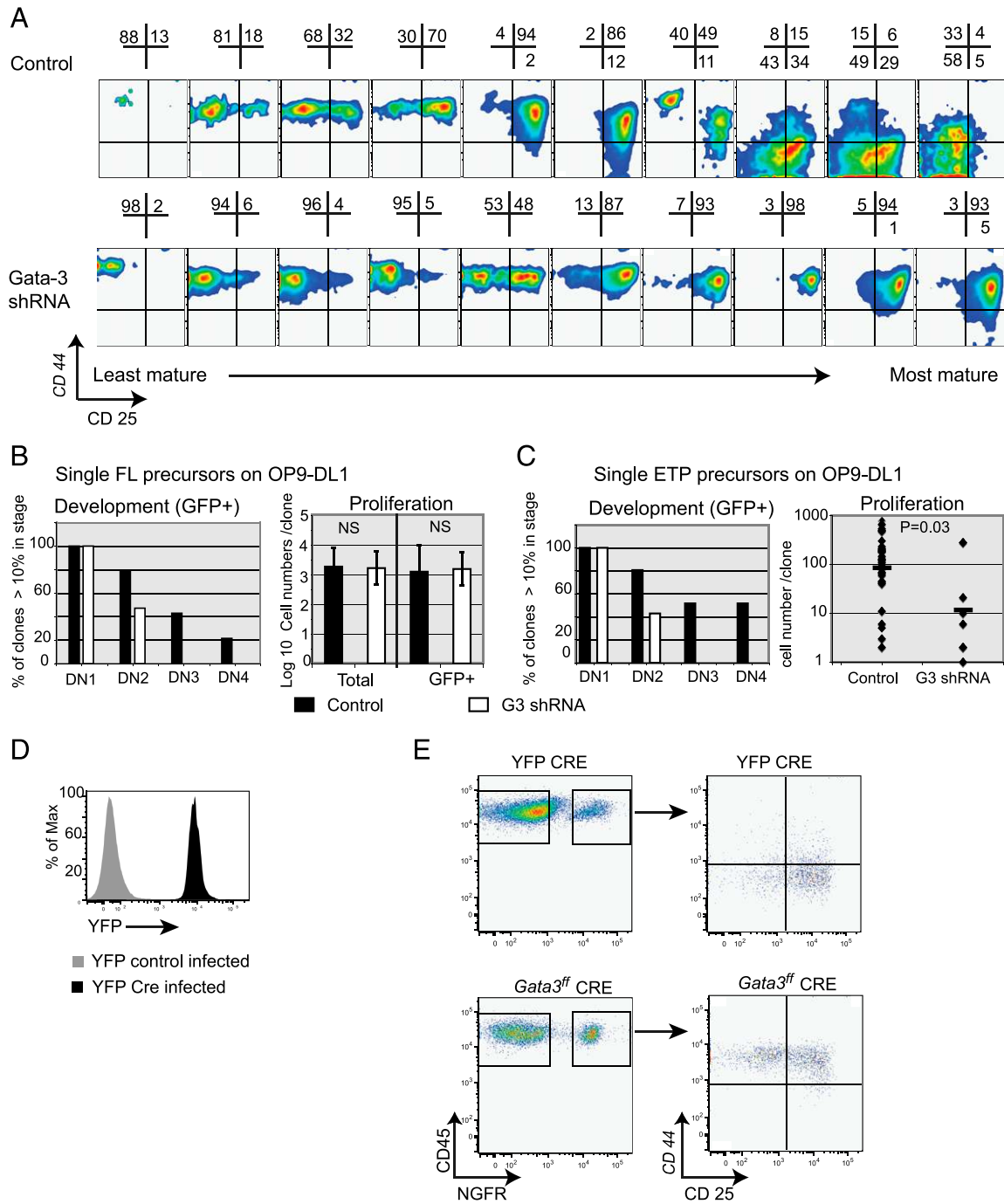


FIGURE 4. Clonal development phenotypes and Cre-mediated deletion phenotypes of GATA-3 loss. **(A)** B6D2F2 FL precursor cells were transduced with empty vector (*top*) or G3-3W (*bottom*), sorted as single cells onto OP9-DL1 monolayers in microtiter wells, and cultured for 8 or 12 d. Phenotype of GFP⁺ descendants is shown, with clones ordered from least development to most (left to right). **(B)** Quantitation of developmental progression and proliferation of FLDN clones shown in (A). Development bar graph (*left*) shows the frequency of clones deriving either from control-infected or G3-3W-infected single cells scored for progression of at least 10% of the GFP⁺ clonal descendants through DN1, DN2, DN3, and DN4 stages, as described in *Materials and Methods*. Total CD45⁺ cell numbers per clone after 8 d culture are shown (*left*) and those remaining GFP⁺ (*right*). **(C)** E14–14.5 B6D2F2 fetal thymic ETPs were infected with G3-3W or control and sorted clonally as described. Quantitation of ETP developmental progression (*left*) and proliferation (*right*) in clonal progeny is shown as in (B). **(D)** FL precursors from *Gata3*^{+/+};*ROSA26R-EYFP* (Cre excision reporter) mice were infected with a Cre-expressing retrovirus. Histogram shows efficient Cre excision to activate the EYFP reporter after 3 d in OP9-control preculture. **(E)** *Gata3*^{fl/fl} and *ROSA26R-EYFP*;*Gata3*^{+/+} FL precursors were induced to express Cre by retroviral transduction during preculture on OP9 control layers as in (D), then sorted for the linked retroviral marker NGFR or for YFP, respectively, and transferred to OP9-DL1 culture for 7 d. Progression is shown for *Gata3*^{fl/fl} and *Gata3*^{+/+} *ROSA26R-EYFP* CRE-expressing cells. Cells in the second column are NGFR gated (representative of two similar experiments; two additional related experiments analyzed at later time points).

tinues, independent of GATA-3 activity levels. At the same time, the split DN2/DN3 phenotype of GATA-3 knockdown cells is a mirror image of our previous finding that when *Gata3*

is overexpressed in fetal thymocytes, c-Kit is upregulated and PU.1 is downregulated (Ref. 14 and Supplemental Figs. 2E, 3G).

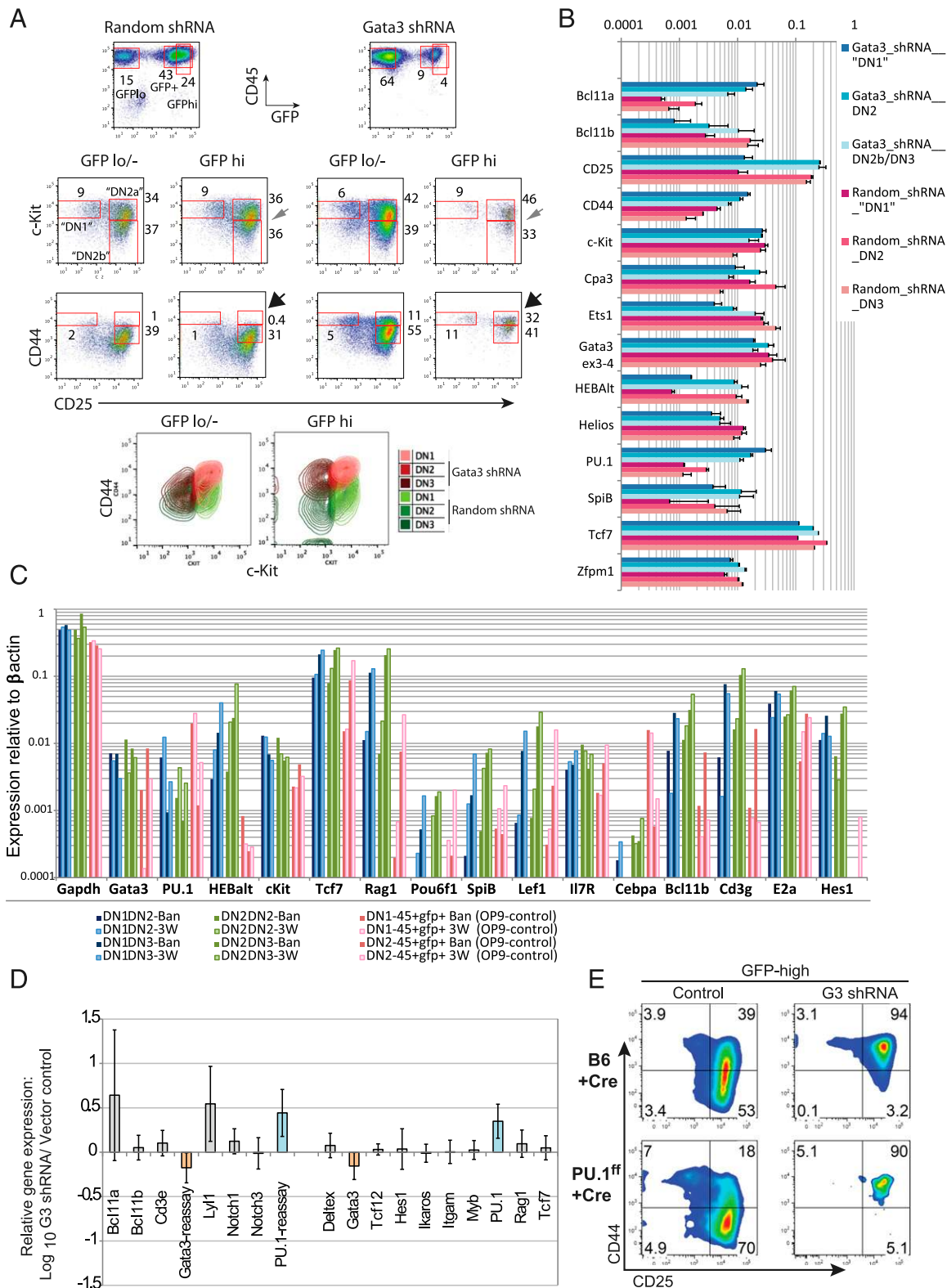


FIGURE 5. Disjunct DN2–DN3 phenotype in GATA-3 knockdown cells. **(A)** Phenotype of DN cells arrested by GATA-3 shRNA is discordant for c-Kit and CD44 expression. Bcl2-transgenic FLPs were transduced with G3-3W or Banshee vector expressing a randomized shRNA sequence and then cocultured with OP9-DL1 for 7 d. Analysis of CD45⁺GFP⁺ cells (*top panels*) after 7 d showed a reduced yield of GFP⁺ and especially GFP^{high} cells from the G3-3W sample (compare Fig. 2G and Fig. 3). *Middle panels*, Phenotypic analysis of gated GFP^{lo/-} cells and the brightest subset of GFP⁺ cells from each sample using CD25 versus c-Kit (*second row*) and CD25 versus CD44 (*third row*). The *fourth row* contour plots show that GATA-3 knockdown caused an elevation of CD44 levels relative to c-Kit levels for all subsets of cells present in the cultures at this time point. Although the DN2-like arrest is evident in terms of CD44 expression, c-Kit expression profiles are much less affected. Numbers are percentages of cells in the indicated gates. Gates used to define GFP^{lo/-}, total GFP⁺, and GFP^{hi} cells are indicated in *top left panel*; gates used to define DN1, DN2a, and DN2b subsets [sorted for analysis (**B**)] are indicated in the *second row of the left panel*. **(B)** Abnormal gene expression in FLDN cells with GATA-3 shRNA in DN2-like arrest. Cells from (**A**) were sorted into DN1, DN2a, and DN2b-like fractions based on CD25 and c-Kit expression to test the possibility that GATA-3 (*Figure legend continues*)

GATA-3 is epistatic to PU.1 in regulating DN2–DN3 progression

PU.1 and GATA-3 act as antagonists in a network circuit in which GATA-3 restrains the ability of PU.1 to cause myeloid differentiation of DN pro-T cells, even when *Spi1* itself is exogenously expressed and not under GATA-3 control (43). PU.1 protein naturally begins at high levels in ETP and DN2a cells, but falls immediately after GATA-3 reaches its peak (data not shown) (42), and our results suggested that GATA-3 might be required for this decline. CD44 that defines the DN2 arrest also appears to be positively regulated by PU.1 (A. Champhekar, unpublished results). To test whether sustained PU.1 expression is the cause of the DN2–DN3 abnormality that occurs when GATA-3 levels are reduced, we asked whether deletion of PU.1 would restore normal development of GATA-3 knockdown FL precursors. Taking FL precursors from *Spi1^{fl/fl}* mice and B6 controls, we treated them in parallel with retroviral Cre to delete PU.1 from the mutant precursors and placed them in T cell differentiation culture for 5 d. Then PU.1-deficient and control cultures were harvested, infected with G3-3W or empty vector, sorted to isolate transduced ETP cells, and these were returned to culture for 7 d more. Fig. 5E shows that loss of PU.1 indeed accelerated the progression from ETP to DN3 in cells with normal levels of GATA-3. However, knocking down GATA-3 still blocked development at DN2, with or without an intact *Spi1* gene. Therefore, the need for GATA-3 to promote DN2–DN3 progression involves additional target genes besides PU.1.

Acute deletion of Gata3 reveals additional GATA-3-sensitive targets

Overall, the relatively modest gene expression effects seen at early time points raised the concern that shRNA-mediated inhibition could be too slow, quantitatively mild, or asynchronous to detect the whole first tier of GATA-3 regulatory targets. For closer study of early responses to GATA-3 deprivation, we therefore used retroviral Cre transduction of cells from homozygous *Gata3^{fl/fl}*; *ROSA26R-YFP* mice and sorted the YFP⁺ DN1, DN2a, and DN2b cells for analysis within 18 ± 2 h, before viability or proliferation-based selection could skew the population (Fig. 6A). These cells were compared with empty vector-infected cells or Cre-treated YFP⁺ cells from *Gata3^{+/+}*; *ROSA26R-EYFP* mice as controls. The level of *Gata3* RNA from the intact floxed gene was reduced by >10-fold by Cre treatment, as determined by exons 3–4-specific qPCR (Fig. 6B). In these cells, within the first day, again *Spi1* (PU.1) was upregulated. However, in contrast to cells transduced with *Gata3* shRNA, now *Zfpml1* (FOG1) was clearly downregulated. This was significant because *Zfpml1* exhibits strong binding of GATA-3 in vivo (13) and seems responsive to GATA-3 in a model cell line system (43). When incubation was continued for an ad-

ditional day before harvesting the cells, detectable reductions in *Tcf7*, *Rag1*, *Kit*, and *Zbtb16* (PLZF) were seen, as well as effects on *Bcl11b* and *Ets1* (Fig. 6B). These effects suggest that such targets associated with particularly strong binding of GATA-3 in vivo (13) may require >2- to 3-fold reductions of GATA-3 activity before their expression is affected.

Global analysis of GATA-3-dependent genes in DN2 cells by RNA-seq

These results suggested that additional immediate targets of *Gata3* in thymocytes undergoing commitment might be found in a whole-genome screen using the acute deletion strategy. We therefore carried out exploratory genome-wide analyses of control and acutely *Gata3*-deleted DN2 cells using RNA-seq. The Cre-transduced FLDN2 cells from *Gata3^{fl/fl}*; *ROSA26R-EYFP*⁺ mice were sorted ~18 h after transduction in two independent experiments, compared in each case with a different control that had been cultured in parallel: in one, Cre-treated cells from B6 mice (wild-type *Gata3*), and in the other, vector marker-positive cells from *Gata3^{fl/fl}*; *ROSA26R-EYFP* mice transduced with an empty vector. At this very early time point, there were no detectable differences yet in viability, cell number, or phenotype between the *Gata3*-deleted and control cells in either experiment (data not shown), but sequences from *Gata3* exons 4 and 5 were effectively eliminated from the transcript repertoire of the Cre⁺ *Gata3^{fl/fl}* cells (Fig. 6C). Transcriptome analyses were carried out using high-throughput sequencing, and gene expression was mapped and quantitated using TopHat and Cufflinks software.

The data were monitored first to establish the global developmental stages that each sample best represented. Catching the cells at identical points even in a normal developmental trajectory is difficult in independent experiments. Overall, the expression patterns agreed well across the four samples (9580 transcripts scored), with Pearson's *r* values of 0.90–0.96 between all pairwise comparisons. To gain a finer mapping of the cells' developmental positions, we established a reference list of 173 developmentally regulated transcription factors from our previous analysis of wild-type cells (13) to create a high-dimensional metric of any sample's advancement through the commitment process. The expression levels of these genes were then used for principal component analysis (Fig. 6D, Supplemental Table IA) of 11 samples from previously defined T cell developmental stages in comparison with the new GATA-3 knockout samples and controls. The first two principal components explained >85% of the total variance among the samples and established a strong canonical trajectory for normal development from FLDN1 through FLDN2a, FLDN2b, and the thymic DN3a to thymic CD4⁺CD8⁺ stage. As shown in Fig. 6D, expression values of the index genes in the new controls placed them appropriately between the FLDN2a and FLDN2b stages. The values for the two GATA-3 knockout samples showed them close to

knockdown simply caused a skewed CD44 surface phenotype. Results are shown from qPCR analysis with indicated genes. GATA-3 knockdown cells are well matched with controls in c-Kit, CD25, and other features of gene expression, but substantially skewed toward an immature profile in terms of reduced *Bcl11b* and *Ets1* expression and overexpressed PU.1 and *Bcl11a* as well as CD44. Data were compiled from two independent experiments, except for *Tcf7*, measured in one, which is shown for reference. Bars show geometric mean values; error bars indicate half-range. (C) *Bcl-2*-transgenic FLDN cells were transduced with Banshee or G3-3W, sorted as GFP⁺ DN1 and DN2 subsets, and then each was recultured for 60 h on OP9-DL1 prior to resorting DN2 and DN3 progeny for RNA analysis (blue bars indicate DN2 and DN3 progeny of DN1 cells; green bars indicate DN2 and DN3 progeny of DN2 cells). In parallel, aliquots of each parental DN1 and DN2 sample were recultured for 60 h on OP9-control and resorted to collect all GFP⁺CD45⁺ progeny (red bars as indicated) to examine the effect of GATA-3 on maintenance of T lineage genes in the absence of DL1. (D) *Bcl-2*-transgenic E15.5 fetal thymocytes were transduced with Banshee or G3-3W overnight, transferred to OP9-DL1, and then Thy1⁺GFP⁺ cells were sorted after 24 h more (40 h total) for gene expression analysis. qPCR analysis was done in two batches with *Spi1* (PU.1) and *Gata3* in both. Gene expression normalized to β-actin is shown as log₁₀ (G3-3W value/Banshee value). Blue shaded bars, *p* < 0.05. Orange shading indicates *Gata3*. (E) PU.1 deficiency does not rescue the DN2–DN3 block in *Gata3* shRNA-transduced cells. E14.5 FL precursors from *PU.1^{fl/fl}* or B6 mice were infected with Cre retrovirus, and Cre⁺-c-Kit⁺CD27⁺ cells were sorted for culture with OP9-DL1. On day 5, DN cells from these cultures were transduced with G3-3W or Banshee empty vector, and GFP ETP cells were sorted the next day and then returned to culture on OP9-DL1. Staining profiles of GFP^{hi} cells are shown after 7 further days of culture.

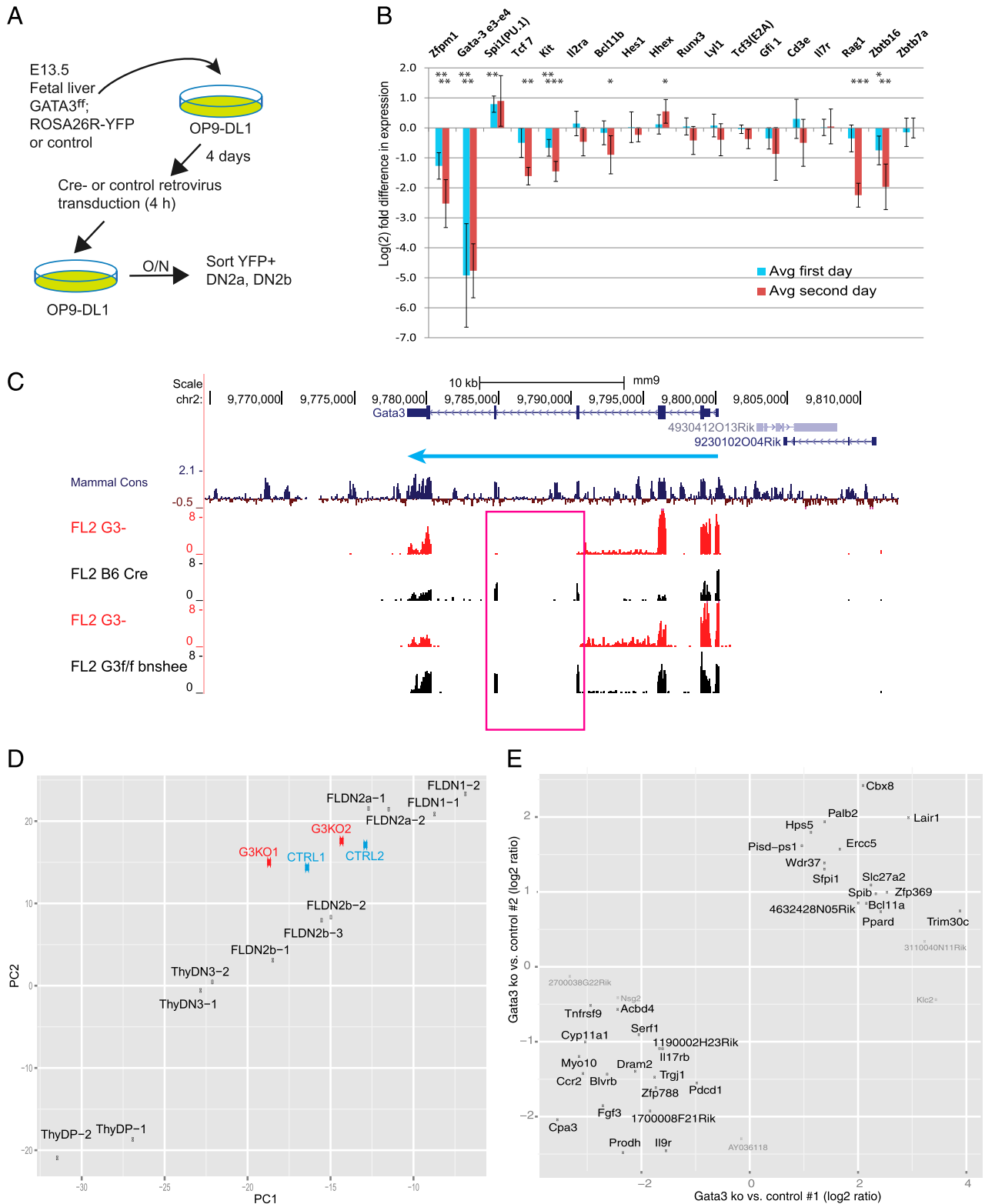


FIGURE 6. RNA-seq analysis of acute responses to *Gata3* deletion. **(A)** Schematic of experimental strategy for generating samples to analyze acute short-term impacts of *Gata3* deletion. In all experiments, *Gata3*-deleted cells were generated by retroviral Cre transduction of *Gata3*^{ff}; *ROSA26R-EYFP*⁺ FL precursors. In two of the three experiments used for the graph in **(B)**, controls were *Gata3*^{+/+}; *ROSA26R-EYFP*⁺ FL cells also transduced with Cre. In a third experiment and RNA-seq samples shown in **(C)**–**(E)**, one control was B6 transduced with Cre (~50% of sorted DN2 cells were transduced), and the other control was *Gata3*^{ff} transduced with empty Banshee vector and sorted for GFP⁺. **(B)** Changes in expression of key genes in the first 16–40 h after deletion of *Gata3* exons 4–5. Cells sorted immediately as shown in **(A)** (first day) or returned to OP9-DL1 coculture for 22–24 more hours (second day) and resorted were analyzed by qPCR for the expression of the indicated genes. Levels are shown on a log₂ scale relative to levels of β-actin. Averages (±SD) of log₂-transformed data from three independent experiments are shown in which values were measured separately for cells sorted as DN2a and cells sorted as DN2b. Significant *p* values for first day (above) and second day (below) differences are shown separately (two-tailed *t* test with unequal variances on difference values). **p* < 0.05, ***p* < 0.005, ****p* < 0.001. **(C)** RNA-seq tracks showing complete deletion of exons 4 and 5 (*Figure legend continues*)

their respective controls, but displaced from the normal trajectory, in parallel. This was consistent with the interpretation that the effects of *Gata3* deletion are not simply a developmental block or acceleration of the normal program, but a deviation from it.

To locate candidates for new GATA-3-sensitive genes, we ranked the genes with greatest differences between controls and experimental samples in both experiments, using both rank product and Cuffdiff analyses with a cutoff to exclude genes expressed at very low levels, as described in *Materials and Methods* (Supplemental Table IB–D). In general, at the time point analyzed (~18 h of Cre exposure), most expression differences were still small, limiting statistical power. However, the limited comparison still revealed ~100 genes of most interest (Supplemental Table IC), and fold changes in expression values in the two comparisons for the top scoring genes are shown in Fig. 6E. Although genes detected as differentially regulated by qPCR (compare Fig. 5B–D and Fig. 6B) also behaved consistently in this RNA-seq analysis (e.g., *Ets1*, *Bcl11b*, *Zbtb16*, *Rag1*), most did not show the strongest effects statistically. However, *Spi1* (PU.1), *SpiB*, and *Bcl11a* were found among the most upregulated in these *Gata3*-deficient DN2 cells (Fig. 6E), supporting the interpretation that these are directly or indirectly repressed in normal DN2 cells by GATA-3.

The top candidates for GATA-3⁺ regulatory targets included genes known to play roles in Th2 cell development, innate lymphocyte type 2 (ILC2) development, and allergic disease, albeit not previously known to be involved in early pro-T cell specification. A highly GATA-3-dependent gene, *Cpa3*, had previously been shown to be upregulated when fetal thymocytes overexpressed GATA-3 (14). These comparisons showed strong effects also on *Il9r*, *Il17rb* (IL-25R component), *Fgf3*, *Tnfrsf9* (4-1BB, CD137), *Cyp11a1*, and germline transcripts of the TCR γ C1 cluster. *Il9r*, *Il17rb*, *Tnfrsf9*, *Pdcd1*, and *Cyp11a1* are also genes recently shown to be positively regulated by GATA-3 in ILC2 and/or Th2 cells (12, 47, 48), as well as *Il17rb*, *Pdcd1*, and *Ms4a4b* in ILC3 or Th17 cells (12, 47). In contrast, the genes appearing as negative regulation targets in our cells do not generally appear GATA-3 regulated in Th2 or ILC2 cells (with the exception of *Lair1*), mostly because they are completely silent in those developmental contexts. Although not all of the genes affected in our analysis are necessarily direct targets (see *Discussion*), they reveal some commonalities in GATA-3 targets between early pro-T cells and peripheral Th2 and ILC2 cells (47–49).

GATA-3 as a positive and negative regulator of other developmental regulatory factors

Because genes of most interest to explain developmental changes prominently include those encoding transcription factors, we specifically examined the impacts of *Gata3* deletion on a genome-wide list of transcriptional regulatory genes (Supplemental Table IE, IF). From a master list of 1640 regulators (Supplemental Table IF, list 1), 973 were expressed highly enough to evaluate (Supplemental

Table IF, lists 2 and 3). To accommodate the variation in starting developmental states in the two comparisons, we used two scoring systems to identify genes of interest (Supplemental Table IE) based on consistency of the *Gata3* deletion effect, minimum fold change, agreement between the controls, and overall strength of expression so as to minimize measurement noise. One list was identified using slightly less stringent criteria but adding a requirement for Cuffdiff *p* of <0.1 (Supplemental Table IE, list 1), and the other was identified using more stringent categorical criteria irrespective of the Cuffdiff *p* value (Supplemental Table IE, list 3). In both lists, *Ets1* was scored as a positive target whereas *SpiB* and *Spi1* were scored as negative regulatory targets. *Bcl11b* also crossed the threshold as a positive target in one list, and *Bcl11a* did the same as a negative target. This screen also identified *Pou2f1* (Oct1), *Hmbox1*, *Anks1*, and *Hmga2* as positive regulatory targets of GATA-3 and *Cbx8* and *Bcl13* as additional negative targets. Note that *Zfpml*, *Tcf7*, and *Myb*, also genes with strong GATA-3 binding in vivo, showed weaker but repeated changes consistent with being functionally positive regulatory targets even though they did not rise to the top statistically (Supplemental Table IE, list 2).

The significance of effects on *Pou2f1*, *Hmbox1*, *Anks1*, and *Hmga2* are difficult to evaluate because so little is known about their roles in T cell development. However, the evidence that *Bcl11b* and *Ets1* depend on GATA-3 activity to be induced raises the possibility that these mediate GATA-3 roles in T cell lineage commitment as well as differentiation.

GATA-3 suppresses B cell potential: a commitment role distinct from that of Bcl11b

Full commitment as well as progression from DN2 to DN3 are known to depend on *Bcl11b*, the regulatory gene that is most dramatically activated between DN1 and DN2b in normal cells (20, 50). If GATA-3 mediates commitment effects through induction of *Bcl11b*, then *Bcl11b* knockouts should recapitulate some of those effects in a GATA-3⁺ context (11). However, the effects of *Bcl11b* and GATA-3 on early pro-T cells are not the same in general. Unlike *Gata3*-deleted cells, *Bcl11b* knockout cells are highly viable. They upregulate c-Kit rather than downregulating it, and even after weeks of OP9-DL1 culture remain proliferative, yet are still able to generate NK and myeloid cells when shifted to OP9-control stroma (20). We therefore tested whether the specific roles of GATA-3 and *Bcl11b* in commitment are the same. The results of this series of experiments with FL and bone marrow precursor-derived DN cells are reported in full in Tables II and III.

To characterize the genetic interactions between GATA-3 and *Bcl11b*, we generated doubly floxed *Bcl11b*^{fl/fl}; *Gata3*^{fl/fl} homozygotes. We crossed the ROSA26R-EYFP reporter into both singly and doubly floxed genotypes as a monitor for Cre efficiency. FL precursors from ROSA26R-EYFP control, *Bcl11b*^{fl/fl}, *Gata3*^{fl/fl}, and *Bcl11b*^{fl/fl} *Gata3*^{fl/fl} mice were retrovirally Cre treated, sorted based

from the *Gata3* gene within 1 d of acute Cre treatment. Tracks from the University of California Santa Cruz genome browser view of the *Gata3* gene (mm9) are shown, with the RefSeq structure of the gene (*top*) and the direction of transcription indicated as a blue arrow between the gene model and the sequence conservation track. Red tracks indicate RNA-seq from GATA-3-deleted samples from two RNA-seq experiments. Black tracks indicate RNA-seq from controls in two RNA-seq experiments. The structure of the floxed *Gata3* gene enables Cre to excise exons 4 and 5 (magenta box). Note, however, that transcription of the *Gata3* 5' exons upstream of the deletion actually increases in the *Gata3*-deleted samples. (D) Principal component analysis of overall developmental staging of GATA-3 knockout samples (G3KO1 and G3KO2, red) compared with controls (CTRL1 and CTRL2, blue) based on RNA-seq analysis of expression levels of 173 diagnostic transcription factors (see Supplemental Table 1A). The axes for the principal component analysis were calculated from the expression levels of these factors in samples described in Zhang et al. (13). Overall, the experimental samples are situated between normal FLDN2a and FLDN2b, consistent with the phenotypes and lengths of culture, but the two experiments are not identical. (E) Highest scoring genes affected within 20 h by deletion of *Gata3* in two experiments: genes downregulated by loss of *Gata3* are at *lower left*; genes upregulated by loss of *Gata3* are at *upper right*. Graph shows fold changes in expression relative to controls on log₂ scale with effects seen in comparison 1 on the x-axis and effects seen in comparison 2 on the y-axis. Genes indicated in black are clearly expressed. Names of other genes fulfilling statistical criteria but expressed at very low levels are indicated in gray.

Table II. Summary of the *Bcl11b*^{fl/fl}; *Gata3*^{fl/fl} experiments

	Percentage of DN2 in Primary Culture (FLPs on OP9-DL4)					Percentage of CD19 ⁺ Cells in Secondary Culture (DN2 on OP9-Control)					Comments
	B6 YFP		<i>Bcl11b</i> ^{fl/fl}		<i>Gata3</i> ^{fl/fl}		<i>Bcl11b</i> ^{fl/fl} ; <i>Gata3</i> ^{fl/fl}		<i>Bcl11b</i> ^{fl/fl} ; <i>Gata3</i> ^{fl/fl}		
E5	54	62	33	0.23	0.80	70.30					For details, see Supplemental Fig. 3 Two independent secondary cultures
E6		64.4	8.03		1.89; 3.17	97.7; 93.1					
E7		71.3	17.7		0.0372	16.2					
E17 (A)		75.5	55.2								
E17 (B)	49.8		56.6								
E18	42.5	27.7	33	0	0-0.0125	94.7					For details, see Fig. 7 Frequency of CD19 ⁺ wells
E18				0/96	0/96	1/96					

For primary cultures, FLr precursors were cultured on OP9-DL4 with 5 ng/ml IL7, Flt3L, and SCF for 8–10 d. Then, DN2 cells were cultured on OP9-Mig with 5 ng/ml IL-7 and Flt3L for 7–14 d. Bold indicates substantial yield of CD19⁺ cells.

on their activation of YFP (Fig. 7A), seeded on OP9-DL4 stroma, and compared for subsequent development (Fig. 7C, 7D, Supplemental Fig. 3, and data not shown). With or without *Bcl11b*, *Gata3* loss caused a severe relative reduction in cell yield (Fig. 7B), and downregulation of *c-Kit*, with an increased expression of *CD25*, in contrast to the effects seen when *Bcl11b* is deleted alone (Fig. 7B–D, Supplemental Fig. 3G, and data not shown). In all these populations lacking a *Bcl2* transgene, cells surviving the 7–8 d preculture were biased toward preservation of at least one intact *Gata3* allele (Fig. 7F), and this made the DN2 arrest appear incomplete. However, when DN2 cells were sorted from the Cre-treated cells of all four genotypes (Fig. 7C) and then transferred to OP9-control stroma, they displayed sharply different developmental potentials (Fig. 7D, Supplemental Fig. 3A–D). All genotypes generated NK-like cells consistently (Supplemental Fig. 3A–D, cells staining with NK1.1 plus DX5). However, a new phenotype also emerged from the DN2 cells of genotypes with deleted *Gata3*: profuse blooms of CD19⁺, CD45^{int} B lineage cells (Fig. 7D, 7E, Supplemental Fig. 3H). The cells with a B cell surface phenotype strongly expressed B lineage transcription factors *Ebf1* and *Pax5* and had substantially downregulated T cell genes such as *Thy1*, *Tcf7*, and *TCRβ* germline transcripts (Supplemental Fig. 3I). However, in contrast to normal B cells, these cells expressed *TCRγ* and *TCRδ* transcripts, consistent with their early T lineage origin (Supplemental Fig. 3I). Generation of B cells from such OP9-DL4-cultured, sorted DN2 pro-T cells was never observed with wild-type cells and was barely detectable in any experiments with *Bcl11b* single knockout cells (Table II).

B cells were generated in secondary culture from Cre-treated DN2 cells with a floxed *Gata3* allele, with or without floxed *Bcl11b*, in seven of seven experiments (Tables II, III). However, this was not a uniform trait within the Cre-treated *Gata3*^{fl/fl} DN2 populations. In microtiter cultures seeded with limiting numbers of sorted ROSA26R-EYFP⁺ DN2 precursors of different genotypes, no B cells emerged from B6 control or *Bcl11b* single-knockout cells (Supplemental Fig. 3A, 3B). B cells did emerge from *Gata3* single-knockout or *Gata3*, *Bcl11b* double-knockout cells, but only from a minority of these limiting dilution cultures (Supplemental Fig. 3C, 3D). The colonies containing B cells proliferated strongly, outstripping those with NK cells only (Fig. 7E, red dots versus blue dots).

One explanation for why B cell clones emerged rarely could be that survival pressures caused many Cre⁺ DN2 cells to retain a *Gata3* allele. This proved to be true based on real-time PCR assays that quantitated deleted versus intact (floxed) *Gata3* alleles (Fig. 7F, 7G). Not only the starting populations, but also all “GATA-3 knockout” colonies that grew on OP9-DL4 stroma actually retained one floxed, undeleted *Gata3* allele. Of the colonies that grew on OP9-control, those of NK cells (Fig. 7F, blue symbols) also all retained *Gata3*. The only colonies that had deleted both copies of *Gata3* were the ones that generated B cells (Fig. 7F, red symbols). In contrast, both NK and B cell colonies showed equal, complete deletion of *Bcl11b* when these alleles were floxed (Fig. 7I, 7H). Thus, only by loss of all *Gata3*, irrespective of the presence or absence of *Bcl11b*, could DN2 pro-T cells convert into B cells.

Deletion of *Gata3* at DN2 stage can restore B cell potential

To determine whether GATA-3 itself is needed continuously to suppress B cell potential, we allowed cells to develop to the DN2 stage with *Gata3* intact and then induced deletion with a tamoxifen-inducible Cre-ERT2 transgene. Bone marrow cells from these mice were cultured on OP9-DL4 to the DN2 pro-T cell stage, then treated with tamoxifen, and DN2 cells were purified by sorting (Fig. 8A, 8B). They were then tested for B cell potential by transfer to OP9-control cultures. Short-term activation of Cre-ERT2 did not cause disappearance of the DN3 cells already

Table III. Summary of experiments deleting *Gata3* at the DN2 stage

		Percentage of DN2 in Primary Culture (Bone Marrow-Derived LSK on OP9-DL4)		Percentage of CD19 ⁺ Cells in Secondary Culture (DN2 on OP9-Control)		Comments
		<i>Cre-ERT2</i>	<i>Cre-ERT2;Gata3^{fl/fl}</i>	<i>Cre-ERT2</i>	<i>Cre-ERT2; Gata3^{fl/fl}</i>	
F8	Experiment 1	70.4	91.1	0.07	40.4	For details, see Fig. 8A–C
F11	Experiment 2	78.8	94.3	0.84	92.6	
G2	Experiment 3	85.7	88.3	0/96 wells (MigR1)	2/96 wells (MigR1 vector)	For details, see Fig. 8D–G
				0/96 wells (Bcl-x _L)	17/96 wells (+Bcl-x_L)	

For primary cultures, bone marrow Lin[−]Sca1⁺c-Kit⁺ (LSK) were cultured on OP9-DL4 with 5 ng/ml IL-7 and Flt3L for 11 d. Then, 4OHT was added into the culture for 16 h before DN2 cells were sorted. For secondary cultures, DN2 cells were cultured on OP9-Mig with 5 ng/ml IL-7 and Flt3L for 7–14 d. The secondary culture of G2 is a colony frequency assay. Bold indicates CD19⁺ cells.

generated but changed the potential of the DN2 cells. Again, no B cells developed from control Cre-treated DN2 cells, but B cells consistently grew out from the Cre-treated *Gata3^{fl/fl}* precursors, even though they had harbored an intact *Gata3* gene until the DN2 stage (Fig. 8C).

Despite the strong outgrowth of converted B cells, the B cell precursor frequency within the *Gata3^{fl/fl}* Cre-treated DN2 population was low. Real potential might be masked by the harsh T lineage effects of acute Notch signal deprivation plus the sudden loss of GATA-3, in transition before the cells switch fates. To obtain a clearer estimate of B cell potential, we generated DN2/3 cells from *Gata3^{fl/fl}* Cre-ERT2 and control Cre-ERT2 mouse bone marrow Lin[−]c-Kit⁺Sca1⁺ cells (Fig. 8D, 8E), then infected them with Bcl-x_L or control retroviral vectors (Fig. 8F), and only then treated them overnight with tamoxifen to activate the Cre. The transduced cells were then sorted and transferred to B cell conditions at limiting dilution for 14 d. As shown in Fig. 8G, imposed expression of Bcl-x_L enhanced the detection of B cell precursors in the *Gata3*-deleted population by 5- to 10-fold without unmasking any B cell potential in the controls. Once GATA-3 is induced, therefore, its vital role in survival amplifies its effectiveness as a suppressor of alternative fates.

Dose-dependent effects of GATA-3 on B and myeloid developmental choice

The difference between full GATA-3 expression and GATA-3 dosage reduction can directly contribute to myeloid potential through the GATA-3 sensitivity of PU.1 expression (Figs. 5, 6A) and PU.1 function (43) (data not shown). Although *Gata3* deletion also unmasks B cell potential as late as the DN2 stage (Figs. 7, 8), B cell development was never seen from G3-3W-treated DN pro-T cells, and the experiments shown in Figs. 5 and 6 revealed no significant activation of *Ebfl* or *Pax5* when GATA-3 activity was merely reduced (data not shown). We therefore considered that B cell potential might be particularly easily repressed by low doses of GATA-3. Indeed, FL precursors in which GATA-3 was reduced by either shRNA or siRNA (Fig. 9A, 9B) often generated an absolutely enhanced yield of B lineage cells (CD19⁺) under B cell/myeloid conditions in OP9 control cultures (in 7 of 10 experiments) (Fig. 9C). Conversely, GATA-3 overexpressing FL precursors, even when Bcl2 transgenic, generated dramatically reduced numbers of CD19⁺ and CD11b⁺ cells in B cell/myeloid conditions (Fig. 9A, Gata-3). To test whether GATA-3 may act as a direct repressor of genes that promote B cell fate, we designed a construct that fuses GATA-3 to the repression domain of *Drosophila* engrailed to create an obligate repressor with GATA factor DNA binding specificity. This construct indeed dampens c-Kit expression in early pro-T cells, consistent with the previous evi-

dence that this gene can be positively regulated by GATA-3 (14) (Supplemental Fig. 2E). *Gata3* engrailed mimicked wild-type GATA-3 expression, however, as it inhibited B cell development (*Gata3* engrailed; Fig. 9A, Supplemental Fig. 2D). This effect was particularly striking because *Gata3* engrailed was far less antagonistic to myeloid development from the FL precursors than wild-type GATA-3, implying a sharp difference in the crucial target genes for these two developmental restriction effects (Fig. 9A, right panels).

To test systematically how GATA-3 dose might affect developmental alternatives, we generated a retroviral GATA-3 construct fused through a linker to an estrogen receptor hormone binding domain [GATA-3(ER)]. This construct offers two levels of dose control, the first through downregulation of vector transcription that occurs in some cells (28), and the second through titrated tamoxifen control of nuclear localization of the expressed fusion protein. We transduced FL precursors with this construct, sorted GFP⁺ transductants, then cultured them under B cell- and myeloid-permissive conditions, with and without tamoxifen. With tamoxifen, GATA-3(ER) blocked GFP^{hi} cells from both B and myeloid fates (Fig. 9D and data not shown), especially M-CSF-R⁺ (CD115⁺) and F4/80⁺ macrophages (data not shown). However, generation of CD19⁺ B cells was clearly most sensitive. B cell generation could be inhibited by strong expression of GATA-3(ER) even without tamoxifen (Fig. 9D, GFP^{hi}, and data not shown) through the small fraction of GATA-3 that still leaks to the nucleus in these conditions (A.M. Arias, unpublished data). In this case, myeloid differentiation (CD115⁺) was clearly less affected (Fig. 9D, arrows, and data not shown). GFP^{lo} cells that had downregulated the GATA-3(ER) construct showed a parallel response pattern at higher doses of tamoxifen (relative sparing of myeloid cells: arrows in Fig. 9D, GFP^{hi} versus GFP^{lo}). Thus, as summarized in Fig. 9E, distinct dose thresholds for GATA-3 not only control DN2–DN3 progression but also limit distinct alternatives to T cell fate.

Discussion

GATA-3 has long been recognized as essential for T cell development, and it is expressed with only modest quantitative changes throughout T cell development. We show in the present study that it is profoundly dose-dependent in its action. Important qualitative effects on lineage choice, differentiation, and gene targeting can emerge from increased levels of GATA-3 expression; excess GATA-3 aborts T cell development, even when the excess is small (12, 14, 44). However, in its roles to promote T lineage fates, GATA-3 has been studied exclusively in an all-or-none fashion (3, 7, 10, 11). In this study, we have used a variety of developmental conditions, differing in precursor sources, developmental timings, and durations of perturbation, to reduce GATA-3 dosage, in order to show that the

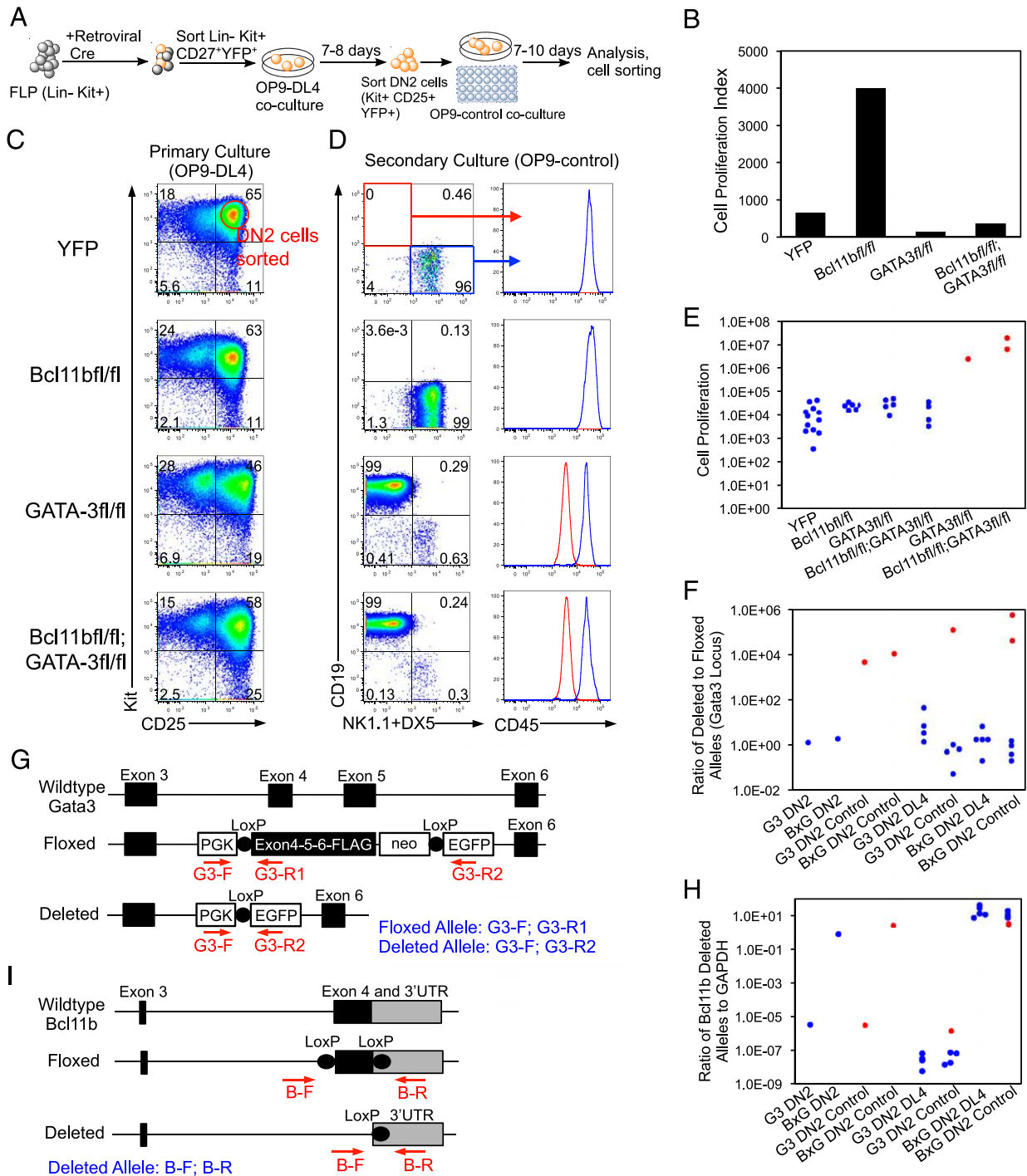


FIGURE 7. Deletion of *Gata3* unleashes B cell potential in FL precursor-derived DN2 cells in the presence or absence of *Bcl11b*. **(A)** Experimental design. Retroviral Cre-infected FLPs from ROSA26R-EYFP (YFP), ROSA26R-EYFP;*Bcl11b*^{fl/fl} (*Bcl11b*^{fl/fl}), ROSA26R-EYFP;*Gata3*^{fl/fl} (*GATA-3*^{fl/fl}), and ROSA26R-EYFP;*Bcl11b*^{fl/fl};*Gata3*^{fl/fl} (*Bcl11b*^{fl/fl};*GATA-3*^{fl/fl}) were all sorted for successful activation of the YFP Cre reporter and cultured on OP9-DL4 for 7–8 d. YFP⁺ DN2 cells were then sorted and split to secondary cultures on OP9-DL4 or OP9-control (OP9-Mig) for 7–14 d more before analysis. **(B)** Cell proliferation of primary cultures on OP9-DL4 in bulk culture. Proliferation index was calculated by dividing the cell numbers of day 7 cultures by the input FLP cell numbers. **(C and D)** Primary culture phenotype and secondary culture outputs of control, *Bcl11b*-deficient, and/or *Gata3*-deficient DN2 cells after treatment with Cre. Deletion of *Gata3* confers gain of alternative function (B cell potential) in *Bcl11b* knockout context. DN2 cells were sorted from 7-d primary cultures as indicated in (C) and analyzed after 7-d secondary cultures on OP9-control stroma. As shown in (D), cells with NK markers developed from *Gata3*⁺ cells, whereas CD19⁺, CD45^{int} B lineage cells developed only from *Gata3* single or double knockout DN2 cells on OP9-control stroma. **(E)** Colony size of CD19⁺ cells developed from both double knockout and single *GATA-3* knockout DN2 cells in limiting dilution (see examples shown in Supplemental Fig. 3A–D): when detected, B cell colonies (red symbols) proliferated more than NK cell colonies (blue colonies). **(F)** Efficiency of *Gata3* deletion from NK (blue symbols) and B (red symbols) colonies growing out in limiting dilution colonies from different *Gata3*, *Bcl11b* genotypes (see Supplemental Fig. 3A–D). qPCR reactions were performed on genomic DNA with primer sets to quantitate deleted *Gata3* and still-intact floxed *Gata3* [see (G)] in samples generated from *Gata3*^{fl/fl} precursors. Plots show the ratio of the deleted allele concentration divided by the floxed allele concentration. A ratio of 1, as in the NK colonies, indicates that as many alleles are undetected as deleted, that is, that the cells are mostly heterozygous. A ratio > 10² indicates that >99% of alleles are deleted. BxG, ROSA26R-EYFP;*Bcl11b*^{fl/fl};*Gata3*^{fl/fl} (*Bcl11b*^{fl/fl};*GATA-3*^{fl/fl}); Control, cultured on OP9-control; DL4, cultured on OP9-DL4; G3, ROSA26R-EYFP;*Gata3*^{fl/fl}. **(G)** (Figure legend continues)

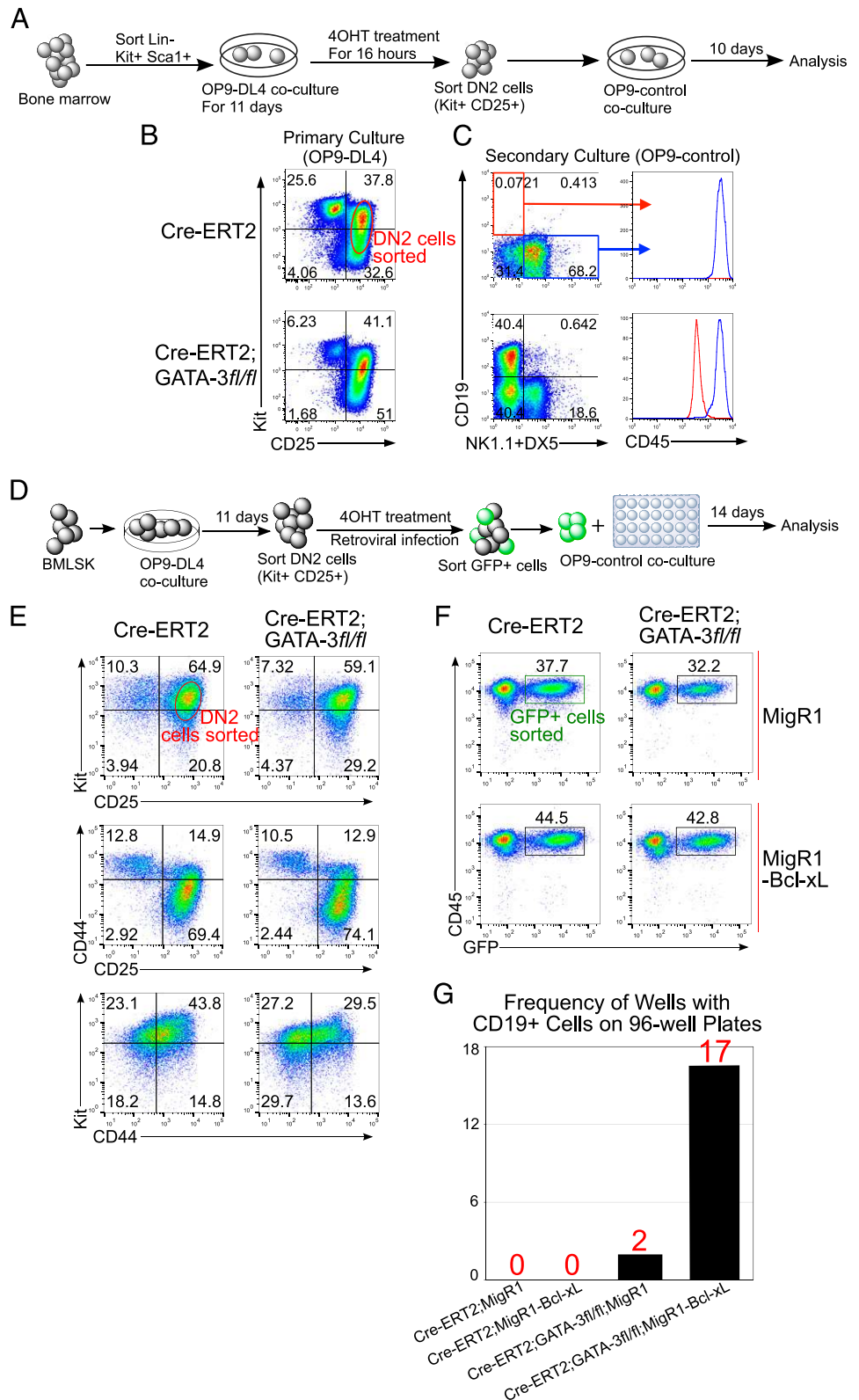


FIGURE 8. Acute deletion of *Gata3* in adult bone marrow LSK-derived DN2 T cells allows B cell development from DN2 T cells. **(A)** Strategy for analysis of B cell potential in pro-T cells when *Gata3* is conditionally deleted only once cells reach DN2 stage using Cre-ERT2 activation by 4OHT 16 h prior to sorting. **(B)** Adult bone marrow LSK-derived DN2 cells were sorted right after 16 h treatment with 4OHT. **(C)** CD19⁺CD45^{int} B cells developed from GATA-3–deleted DN2 cells in secondary culture even when deletion was delayed until DN2 stage. **(D)** Strategy for analysis of the combined effects of *Gata3* deletion and *Bcl-x_L* overexpression in DN2 cells on the emergence of B cells. T lineage differentiation cultures of Cre-ERT2 and *Gata3^{fl/fl}* bone marrow Lin⁻Sca-1⁺c-Kit⁺ cells were followed with acute *Gata3* deletion at DN2 stage by 4OHT-activated Cre and transduction with *Bcl-x_L* or an empty vector. B cell potential of sorted, transduced cells was then assayed by limiting dilution culture on OP9-control stroma. **(E)** Phenotypes and sort gates for DN2 cells before Cre activation. **(F)** Sorting for cells transduced (GFP⁺) with empty vector or *Bcl-x_L* after tamoxifen treatment and retroviral transduction. **(G)** *Bcl-x_L* enhancement of recovery of B cell colonies from converted DN2 cells after acute *Gata3* deletion.

gentle increase in GATA-3 expression from ETP/DN1 stage to DN2b stage can have significant regulatory consequences. First, T cell precursors need GATA-3 to rise beyond its ETP/DN1 level to generate correctly programmed DN2 and DN3 cells. These higher levels of GATA-3 also antagonize PU.1, which may limit myeloid potential. Second, even at low levels, GATA-3 is an acutely sensi-

qPCR primer sets used to measure the deletion of *Gata3* locus used in (F). G3-F/G3-R1 primer set detects the floxed *Gata3* alleles. G3-F/G3-R2 primer set detects deleted *Gata3* alleles. **(H)** Deletion of *Bcl11b* in the samples was measured as in (F), except showing ratio of deleted allele to GAPDH gene signal. The *Bcl11b* deleted product can only be generated from genotypes containing a *Bcl11b* floxed gene (here, BxG), but importantly deletion (*Bcl11b* deleted/GAPDH ratio of >0.1) shows no correlation with NK or B fate of the cells. **(I)** qPCR primer sets used to measure the deletion of *Bcl11b* locus in (H).

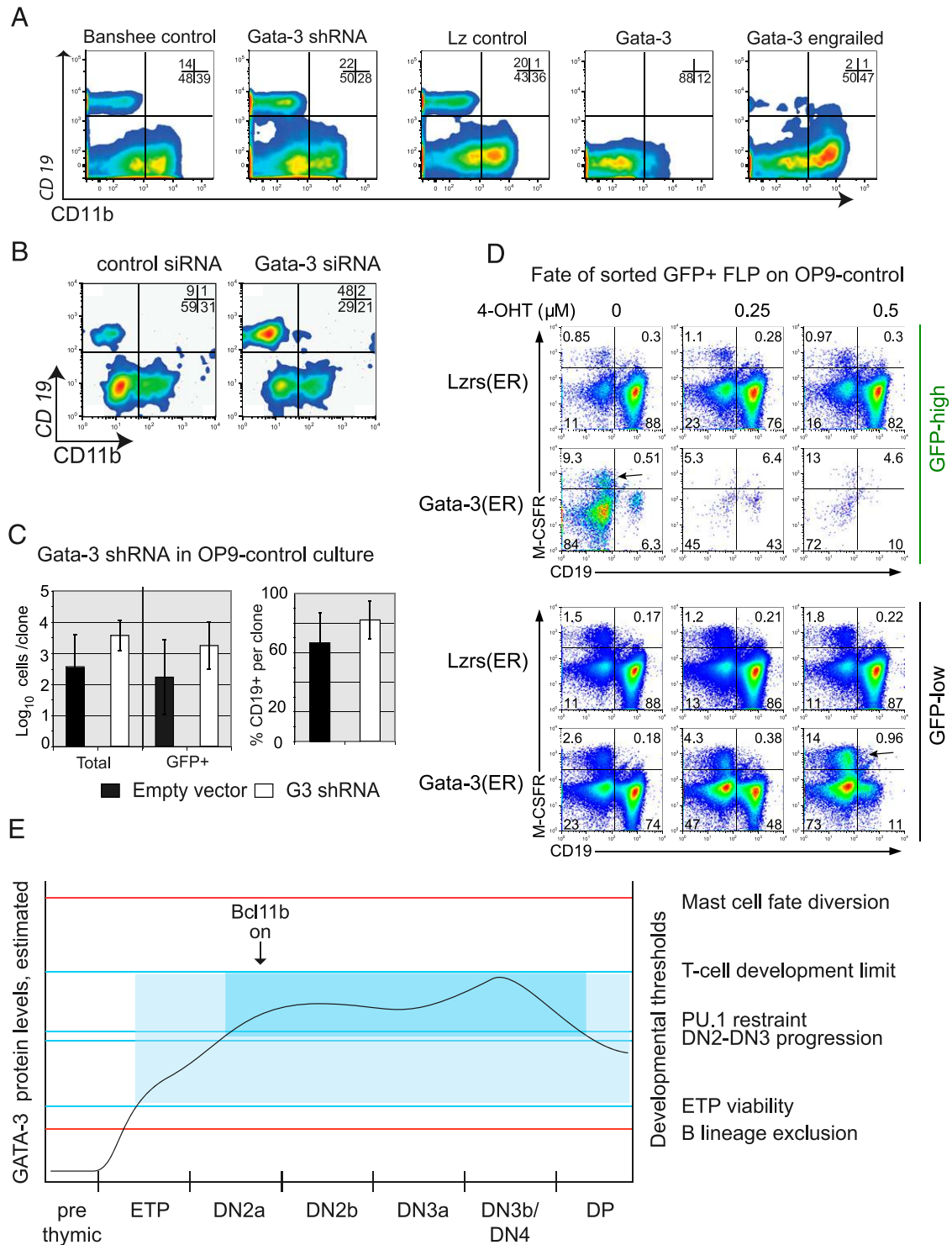


FIGURE 9. Expression of inducible GATA-3 and obligate repressor GATA-3 show distinct mechanisms for GATA-3 inhibition of B and myeloid development. **(A)** GATA-3 knockdown enhances B cell emergence; GATA-3-ENG expression blocks B cell emergence from FLP. Bcl-2-transgenic FL precursors were infected in parallel with either G3-3W or Banshee control constructs, or with retroviral constructs overexpressing normal GATA-3 or an obligate repressor form of GATA-3 (Gata-3 engrailed), or the corresponding vector control (Lz). Sorted FL precursors were then cultured 3.5 d with OP9 control stromal cells (B/myeloid conditions) before analysis (three independent experiments). **(B)** Loss of GATA-3 promotes B cell emergence. FL precursors were nucleofected with siRNA specific for *Gata3*, then sorted and cultured 4–6 d under B/myeloid conditions on OP9 control stroma. Representative data are shown (7 of 10 experiments using nucleofection or retroviral transduction of Gata-3 shRNA). **(C)** B cell recovery from GATA-3 knockdown in clonal precursors. Single FL precursors transduced with Banshee or G3-3W were sorted into 96-well plates with OP9 control stroma and cultured for 12 d. Cell numbers for total cells per clone and GFP⁺ cells per clone are shown for G3-3W and control-infected clones (*left*) (geometric mean \pm SD). Percentages of each clone that were CD19⁺ are shown (*right*). At least as many B cells were generated from cells remaining GFP⁺ after transduction with 3W as with Ban; differences were not statistically significant. **(D)** Dose-dependent hierarchy of B cell and myeloid inhibition by tamoxifen-enhanced GATA-3 [GATA3(ER)]. FL precursors were infected with GATA3(ER) or empty vector [Lz(ER)] and sorted the next day to purify GFP⁺ transductants. GFP⁺ cells were cultured for 6 d on OP9-control in the absence or presence of tamoxifen as indicated. Some CD45⁺ cells continued strong vector expression (GFP^{hi}) whereas others downregulated it (GFP^{lo}). These were analyzed for B (CD19⁺) and myeloid (CD115⁺) development (*Figure legend continues*)

tive repressor of B cell developmental potential. Thus, its early induction in thymic immigrants is properly timed to explain the early exclusion of B cell potential (51) (reviewed in Refs. 52–54).

Dose reduction of GATA-3 by shRNA severely impacted normal population dynamics of DN1 cells and also prevented the development of normal DN2 and DN3 cells from prethymic or DN1/ETP precursors. These effects were initially weak but became increasingly pronounced during a period of days. The surviving DN2 cells with reduced GATA-3 activity were abnormal in several respects, with uncoupling of CD44 and c-Kit regulation and loss of control of both DN1-specific genes and DN3-specific genes. Even with these effects of GATA-3 knockdown, the cells were evidently strongly selected for retention of some residual GATA-3 expression. Cre-mediated deletion of both copies of the *Gata3* gene had catastrophic effects on viability as long as the cells were maintained in Notch-signaling conditions to support T cell development. It was clearly only the cells with full deletion of *Gata3* that reacquired access to the B cell pathway.

Explaining these effects on ETP/DN1 survival, DN2–DN3 progression competence, and access to the B and myeloid fates at a molecular level will require further research, but our results present a wealth of provocative candidate mediators. The early T cell program includes both positive and negative regulatory targets of GATA-3 action, and our results imply that these have different patterns of response to differing degrees of GATA-3 dose reduction. Some genes respond rapidly to any decrease in GATA-3 expression level, and many of these are genes that appear to be relieved from repression when GATA-3 doses drop. Although the magnitudes of the effects are initially modest, these include three genes encoding transcription factors of great developmental significance: the progenitor cell and myeloid regulatory factor PU.1; the closely related factor that collaborates with PU.1 in B cell development, SpiB; and the indispensable lymphoid progenitor factor Bcl11a. The repressive effect of GATA-3 on SpiB supports earlier evidence that SpiB/GATA-3 antagonism can control T cell versus plasmacytoid dendritic cell fate determination in human precursors (55). Likely positive regulatory targets of GATA-3 are less enriched for putative regulatory genes but include genes encoding Ets1 and Bcl11b, two transcription factors that play prominent roles in T lineage commitment and in the DN3 state. However, these genes responded more slowly to the decrease of GATA-3 expression than did *SpiB*, *PU.1*, and *Bcl11a*. Many of the targets most rapidly downregulated by loss of GATA-3 were in fact genes associated with ILC2 cells and mature GATA-3⁺ effector T cells (12, 47, 48), clearly expressed in the normal DN2 cells but not previously associated with early T cell developmental functions. It will be very interesting to determine whether *I19r* and *I117rb* (encoding a chain of the IL-25 receptor) are functionally important in early T lineage development.

ChIP-seq data from two groups have provided maps of GATA-3 binding sites across the genome in thymocytes (12, 13). Unfortunately, these peak patterns in themselves turn out to be poor predictors of the genes most sensitive to acute GATA-3 perturbation. Some likely positive target genes with particularly strong GATA-3 binding such as *Zfpml1*, encoding the GATA factor partner FOG1, were completely insensitive to the shRNA and were only affected by a complete deletion of the *Gata3* gene. More sensitive targets, both positive and negative, were often

only weakly bound by GATA-3 in vivo, when binding was detected at all. Although some of these genes may be indirectly regulated by GATA-3, the very short time points we used were specifically designed to limit indirect effects. Furthermore, the very limited number of transcription factor genes affected at all, and the generally weak effects on those regulatory genes seen at 18–20 h, makes them unlikely candidates for mediating the GATA-3 effects. Thus, although technical factors could be relevant, it is possible that sites with strong GATA-3 occupancy in fact have too high an affinity to be affected by 2- to 3-fold dose reductions. In this case, the molecular mechanisms underlying the potent developmental impact of GATA-3 knockdown must be sought among genes with weak, rapidly exchanging GATA-3 binding sites.

In agreement with our previous results of GATA-3 overexpression, GATA-3 loss of function did not have a clear-cut impact on global Notch signaling; some Notch target genes, including *HEBalt* and *Dtx1*, were even somewhat enhanced in expression. However, there are a number of indirect pathways through which GATA-3 could be collaborating with Notch signals. Our results confirm that GATA-3 is a restraining negative regulator of PU.1 levels in early thymocytes when expressed at its normal physiological level as well as when overexpressed. This means it can protect Notch signaling from PU.1 inhibition and also play a role in the eventual extinction of myeloid potential during commitment. The need for GATA-3 to promote accurate DN2–DN3 progression may also be reflected through its specific importance to induce Bcl11b and Ets1 expression as well. The impact of GATA-3 on ETP/DN1 viability could reflect its positive role in c-Kit gene expression, but our data show that this interpretation can be complicated by the disjunction of c-Kit and CD44 developmental regulation when GATA-3 is removed. Other GATA-3-regulated genes are predicted to encode PHD domain and chromobox chromatin modifiers, which opens a wide range of possibilities for regulating survival and self-renewal. Strikingly, however, the trio of repressed genes *Bcl11a*, *Spi1*, and *SpiB*, whether direct or indirect targets, suggests a pathway through which loss of GATA-3 could simultaneously relieve multiple constraints on the B cell program. It will be of great interest to test these hypotheses.

The distinct dosage thresholds for different critical GATA-3 effects clarify the position of GATA-3 in a T cell commitment network (Fig. 9E). Our results imply that the rising level of GATA-3 first excludes the B cell option, then enables T lineage genes to be turned on, then provides quantitative control over the silencing of PU.1 and myeloid options. Even before helping to activate a definitive T cell program, low-level GATA-3 becomes essential for viability of the earliest T cell precursors. The stage-specific effects of G3-3W shRNA on viability indicate a likely threshold mechanism: even the weak effect of shRNA may push GATA-3 below this threshold when starting from the low levels in ETP/DN1 cells, but not from higher DN2 levels. However, higher, DN2-stage levels of GATA-3 are needed in full to arm cells for competence in developmental progression. Our results confirm that GATA-3 is required to prevent B lineage access, even after T lineage differentiation has begun, through mechanisms that are complementary to, but distinct from, those mediated by Bcl11b (11, 20, 50, 53). In summary, GATA-3 at the DN2 stage is revealed to be a critically dose-dependent regulator of both T lineage progression and unique aspects of T lineage commitment.

(representative of two independent experiments). Concordant results were obtained in an additional experiment under different culture conditions (not shown). (E) Natural changes in GATA-3 levels cross distinct developmental dose thresholds. Schematic of effects from the present study and in other work is shown (3, 7, 11, 14, 44). Red lines indicate thresholds seen in absence of Notch signaling; blue lines, thresholds seen in presence of Notch signaling; light blue zone, permissive for T lineage entry; and darker blue indicates permissive for full T cell commitment.

Acknowledgments

We thank Gabriela Hernandez-Hoyos for the *Gata3* shRNA construct, I-Cheng Ho and Sung-Yun Pai (Brigham and Women's Hospital, Harvard Medical School) for GATA-3-floxed mice, Qiang Tu for advice and help with data deposition, and Barbara Kee (University of Chicago), James Di Santo and Roel Klein Wolterink (Institut Pasteur), and Marcos García-Ojeda (University of California Merced) for stimulating discussions and for sharing data before publication. We thank Christopher Franco and Kira Sarup-Lytzen for assistance with qPCR, Jerry Kwong and Benjamin Park for technical help, and Rochelle Diamond, Stephanie Adams, and Diana Perez for cell sorting. We also thank Frank Costantini (Columbia University), Mark Leid (Oregon State University), Pentao Liu (Cambridge University), and Stephen Nutt (Walter and Eliza Hall Institute) for *ROSA26R-EYFP*, two types of *Bcl11b^{fl/fl}*, and *Sp1^{fl/fl}* founder mice, respectively, Juan Carlos Zúñiga-Pflücker (University of Toronto) for OP9-DL4 cells, and John Rossi (City of Hope), Naoko Arai (DNAX), Tom Taghon (Ghent University), and laboratory members Mark Zarnegar, Sanket Acharya, and Elizabeth-Sharon David-Fung for providing and characterizing retroviral vectors.

Disclosures

The authors have no financial conflicts of interest.

References

- Pandolfi, P. P., M. E. Roth, A. Karis, M. W. Leonard, E. Dzierzak, F. G. Grosveld, J. D. Engel, and M. H. Lindenbaum. 1995. Targeted disruption of the *GATA3* gene causes severe abnormalities in the nervous system and in fetal liver haematopoiesis. *Nat. Genet.* 11: 40–44.
- Ting, C. N., M. C. Olson, K. P. Barton, and J. M. Leiden. 1996. Transcription factor GATA-3 is required for development of the T-cell lineage. *Nature* 384: 474–478.
- Hendriks, R. W., M. C. Nawijn, J. D. Engel, H. van Doorninck, F. Grosveld, and A. Karis. 1999. Expression of the transcription factor GATA-3 is required for the development of the earliest T cell progenitors and correlates with stages of cellular proliferation in the thymus. *Eur. J. Immunol.* 29: 1912–1918.
- Vosshenrich, C. A., M. E. Garcia-Ojeda, S. I. Samson-Villeger, V. Pasqualetto, L. Enault, O. Richard-Le Goff, E. Corcuff, D. Guy-Grand, B. Rocha, A. Cumano, et al. 2006. A thymic pathway of mouse natural killer cell development characterized by expression of GATA-3 and CD127. *Nat. Immunol.* 7: 1217–1224.
- Samson, S. I., O. Richard, M. Tavian, T. Ranson, C. A. Vosshenrich, F. Colucci, J. Buer, F. Grosveld, I. Godin, and J. P. Di Santo. 2003. GATA-3 promotes maturation, IFN- γ production, and liver-specific homing of NK cells. *Immunity* 19: 701–711.
- Hattori, N., H. Kawamoto, S. Fujimoto, K. Kuno, and Y. Katsura. 1996. Involvement of transcription factors TCF-1 and GATA-3 in the initiation of the earliest step of T cell development in the thymus. *J. Exp. Med.* 184: 1137–1147.
- Hosoya, T., T. Kuroha, T. Moriguchi, D. Cummings, I. Maillard, K. C. Lim, and J. D. Engel. 2009. GATA-3 is required for early T lineage progenitor development. *J. Exp. Med.* 206: 2987–3000.
- Ku, C. J., T. Hosoya, I. Maillard, and J. D. Engel. 2012. GATA-3 regulates hematopoietic stem cell maintenance and cell-cycle entry. *Blood* 119: 2242–2251.
- Buza-Vidas, N., S. Duarte, S. Luc, T. Bouriez-Jones, P. S. Woll, and S. E. Jacobsen. 2011. GATA3 is redundant for maintenance and self-renewal of hematopoietic stem cells. *Blood* 118: 1291–1293.
- Pai, S. Y., M. L. Truitt, C. N. Ting, J. M. Leiden, L. H. Glimcher, and I. C. Ho. 2003. Critical roles for transcription factor GATA-3 in thymocyte development. *Immunity* 19: 863–875.
- García-Ojeda, M. E., R. G. Klein Wolterink, F. Lemaître, O. Richard-Le Goff, M. Hasan, R. W. Hendriks, A. Cumano, and J. P. Di Santo. 2013. GATA-3 promotes T cell specification by repressing B cell potential in pro-T cells in mice. *Blood* 121: 1749–1759.
- Wei, G., B. J. Abraham, R. Yagi, R. Jothi, K. Cui, S. Sharma, L. Narlikar, D. L. Northrup, Q. Tang, W. E. Paul, et al. 2011. Genome-wide analyses of transcription factor GATA3-mediated gene regulation in distinct T cell types. *Immunity* 35: 299–311.
- Zhang, J. A., A. Mortazavi, B. A. Williams, B. J. Wold, and E. V. Rothenberg. 2012. Dynamic transformations of genome-wide epigenetic marking and transcriptional control establish T cell identity. *Cell* 149: 467–482.
- Taghon, T. M., A. Yui, and E. V. Rothenberg. 2007. Mast cell lineage diversion of T lineage precursors by the essential T cell transcription factor GATA-3. *Nat. Immunol.* 8: 845–855.
- Schmitt, T. M., and J. C. Zúñiga-Pflücker. 2002. Induction of T cell development from hematopoietic progenitor cells by Delta-like-1 in vitro. *Immunity* 17: 749–756.
- Taghon, T. N., E. S. David, J. C. Zúñiga-Pflücker, and E. V. Rothenberg. 2005. Delayed, asynchronous, and reversible T-lineage specification induced by Notch/Delta signaling. *Genes Dev.* 19: 965–978.

- Strasser, A., A. W. Harris, and S. Cory. 1991. *bcl-2* transgene inhibits T cell death and perturbs thymic self-censorship. *Cell* 67: 889–899.
- Srinivas, S., T. Watanabe, C. S. Lin, C. M. William, Y. Tanabe, T. M. Jessell, and F. Costantini. 2001. Cre reporter strains produced by targeted insertion of EYFP and ECFP into the *ROSA26* locus. *BMC Dev. Biol.* 1: 4.
- Nutt, S. L., D. Metcalf, A. D'Amico, M. Polli, and L. Wu. 2005. Dynamic regulation of PU.1 expression in multipotent hematopoietic progenitors. *J. Exp. Med.* 201: 221–231.
- Li, L., M. Leid, and E. V. Rothenberg. 2010. An early T cell lineage commitment checkpoint dependent on the transcription factor *Bcl11b*. *Science* 329: 89–93.
- Li, P., S. Burke, J. Wang, X. Chen, M. Ortiz, S. C. Lee, D. Lu, L. Campos, D. Goulding, B. L. Ng, et al. 2010. Reprogramming of T cells to natural killer-like cells upon *Bcl11b* deletion. *Science* 329: 85–89.
- Carleton, M., N. R. Ruetsch, M. A. Berger, M. Rhodes, S. Kaptik, and D. L. Wiest. 1999. Signals transduced by CD3 ϵ , but not by surface pre-TCR complexes, are able to induce maturation of an early thymic lymphoma in vitro. *J. Immunol.* 163: 2576–2585.
- Dionne, C. J., K. Y. Tse, A. H. Weiss, C. B. Franco, D. L. Wiest, M. K. Anderson, and E. V. Rothenberg. 2005. Subversion of T lineage commitment by PU.1 in a clonal cell line system. *Dev. Biol.* 280: 448–466.
- Mohshami, M., D. K. Shah, H. Nakase, K. Kianizad, H. T. Petrie, and J. C. Zúñiga-Pflücker. 2010. Direct comparison of Dll1- and Dll4-mediated Notch activation levels shows differential lymphomyeloid lineage commitment outcomes. *J. Immunol.* 185: 867–876.
- Franco, C. B., D. D. Scripture-Adams, I. Proekt, T. Taghon, A. H. Weiss, M. A. Yui, S. L. Adams, R. A. Diamond, and E. V. Rothenberg. 2006. Notch/Delta signaling constrains reengineering of pro-T cells by PU.1. *Proc. Natl. Acad. Sci. USA* 103: 11993–11998.
- Hernandez-Hoyos, G., M. K. Anderson, C. Wang, E. V. Rothenberg, and J. Alberola-Ila. 2003. GATA-3 expression is controlled by TCR signals and regulates CD4/CD8 differentiation. *Immunity* 19: 83–94.
- Hernandez-Hoyos, G., and J. Alberola-Ila. 2005. Analysis of T-cell development by using short interfering RNA to knock down protein expression. *Methods Enzymol.* 392: 199–217.
- Anderson, M. K., G. Hernandez-Hoyos, C. J. Dionne, A. M. Arias, D. Chen, and E. V. Rothenberg. 2002. Definition of regulatory network elements for T cell development by perturbation analysis with PU.1 and GATA-3. *Dev. Biol.* 246: 103–121.
- Kurata, H., H. J. Lee, A. O'Garra, and N. Arai. 1999. Ectopic expression of activated Stat6 induces the expression of Th2-specific cytokines and transcription factors in developing Th1 cells. *Immunity* 11: 677–688.
- Zarnegar, M. A., J. Chen, and E. V. Rothenberg. 2010. Cell-type-specific activation and repression of PU.1 by a complex of discrete, functionally specialized cis-regulatory elements. *Mol. Cell. Biol.* 30: 4922–4939.
- David-Fung, E. S., R. Butler, G. Buzi, M. A. Yui, R. A. Diamond, M. K. Anderson, L. Rowen, and E. V. Rothenberg. 2009. Transcription factor expression dynamics of early T-lymphocyte specification and commitment. *Dev. Biol.* 325: 444–467.
- Trapnell, C., D. G. Hendrickson, M. Sauvageau, L. Goff, J. L. Rinn, and L. Pachter. 2013. Differential analysis of gene regulation at transcript resolution with RNA-seq. *Nat. Biotechnol.* 31: 46–53.
- Breitling, R., P. Armengaud, A. Amtmann, and P. Herzyk. 2004. Rank products: a simple, yet powerful, new method to detect differentially regulated genes in replicated microarray experiments. *FEBS Lett.* 573: 83–92.
- Igarashi, H., S. C. Gregory, T. Yokota, N. Sakaguchi, and P. W. Kincade. 2002. Transcription from the *RAG1* locus marks the earliest lymphocyte progenitors in bone marrow. *Immunity* 17: 117–130.
- Tydel, C. C., E. S. David-Fung, J. E. Moore, L. Rowen, T. Taghon, and E. V. Rothenberg. 2007. Molecular dissection of prethymic progenitor entry into the T lymphocyte developmental pathway. *J. Immunol.* 179: 421–438.
- Tabrizifard, S., A. Orlaru, J. Plotkin, M. Fallahi-Sichani, F. Livak, and H. T. Petrie. 2004. Analysis of transcription factor expression during discrete stages of postnatal thymocyte differentiation. *J. Immunol.* 173: 1094–1102.
- Shinnakasu, R., M. Yamashita, M. Kuwahara, H. Hosokawa, A. Hasegawa, S. Motohashi, and T. Nakayama. 2008. Gfi1-mediated stabilization of GATA3 protein is required for Th2 cell differentiation. *J. Biol. Chem.* 283: 28216–28225.
- Maneechotesuwan, K., Y. Xin, K. Ito, E. Jazrawi, K. Y. Lee, O. S. Usmani, P. J. Barnes, and I. M. Adcock. 2007. Regulation of Th2 cytokine genes by p38 MAPK-mediated phosphorylation of GATA-3. *J. Immunol.* 178: 2491–2498.
- Cook, K. D., and J. Miller. 2010. TCR-dependent translational control of GATA-3 enhances Th2 differentiation. *J. Immunol.* 185: 3209–3216.
- Gimferrer, I., T. Hu, A. Simmons, C. Wang, A. Souabni, M. Busslinger, T. P. Bender, G. Hernandez-Hoyos, and J. Alberola-Ila. 2011. Regulation of GATA-3 expression during CD4 lineage differentiation. *J. Immunol.* 186: 3892–3898.
- Frelin, C., R. Herrington, S. Janmohamed, M. Barbara, G. Tran, C. J. Paige, P. Benveniste, J. C. Zúñiga-Pflücker, A. Souabni, M. Busslinger, and N. N. Iscove. 2013. GATA-3 regulates the self-renewal of long-term hematopoietic stem cells. *Nat. Immunol.* 14: 1037–1044.
- Yui, M. A., N. Feng, and E. V. Rothenberg. 2010. Fine-scale staging of T cell lineage commitment in adult mouse thymus. *J. Immunol.* 185: 284–293.
- Del Real, M. M., and E. V. Rothenberg. 2013. Architecture of a lymphomyeloid developmental switch controlled by PU.1, Notch, and GATA-3. *Development* 140: 1207–1219.
- Xu, W., T. Carr, K. Ramirez, S. McGregor, M. Sigvardsson, and B. L. Kee. 2013. E2A transcription factors limit expression of Gata3 to facilitate T lymphocyte lineage commitment. *Blood* 121: 1534–1542.

45. Kim, D. H., and J. J. Rossi. 2009. Overview of gene silencing by RNA interference. *Curr. Protoc. Nucleic Acid Chem.* Chapter 16: Unit 16.1. doi:10.1002/0471142700.nc1601s36
46. Wang, D., C. L. Claus, G. Vaccarelli, M. Braunstein, T. M. Schmitt, J. C. Zúñiga-Pflücker, E. V. Rothenberg, and M. K. Anderson. 2006. The basic helix-loop-helix transcription factor HEBAlt is expressed in pro-T cells and enhances the generation of T cell precursors. *J. Immunol.* 177: 109–119.
47. Yagi, R., C. Zhong, D. L. Northrup, F. Yu, N. Bouladoux, S. Spencer, G. Hu, L. Barron, S. Sharma, T. Nakayama, et al. 2014. The transcription factor GATA3 is critical for the development of all IL-7R α -expressing innate lymphoid cells. *Immunity* 40: 378–388.
48. Sasaki, T., A. Onodera, H. Hosokawa, Y. Watanabe, S. Horiuchi, J. Yamashita, H. Tanaka, Y. Ogawa, Y. Suzuki, and T. Nakayama. 2013. Genome-wide gene expression profiling revealed a critical role for GATA3 in the maintenance of the Th2 cell identity. *PLoS ONE* 8: e66468.
49. Mahata, B., X. Zhang, A. A. Kolodziejczyk, V. Proserpio, L. Haim-Vilmsky, A. E. Taylor, D. Hebenstreit, F. A. Dingler, V. Moignard, B. Göttgens, et al. 2014. Single-cell RNA sequencing reveals T helper cells synthesizing steroids de novo to contribute to immune homeostasis. *Cell Reports* 7: 1130–1142.
50. Ikawa, T., S. Hirose, K. Masuda, K. Kakugawa, R. Satoh, A. Shibano-Satoh, R. Kominami, Y. Katsura, and H. Kawamoto. 2010. An essential developmental checkpoint for production of the T cell lineage. *Science* 329: 93–96.
51. Heinzl, K., C. Benz, V. C. Martins, I. D. Haidl, and C. C. Bleul. 2007. Bone marrow-derived hemopoietic precursors commit to the T cell lineage only after arrival in the thymic microenvironment. *J. Immunol.* 178: 858–868.
52. Rothenberg, E. V. 2011. T cell lineage commitment: identity and renunciation. *J. Immunol.* 186: 6649–6655.
53. Klein Wolterink, R. G., M. E. Garcia-Ojeda, C. A. Vosshenrich, R. W. Hendriks, and J. P. Di Santo. 2010. The intrathymic crossroads of T and NK cell differentiation. *Immunol. Rev.* 238: 126–137.
54. Yang, Q., J. Jeremiah Bell, and A. Bhandoola. 2010. T-cell lineage determination. *Immunol. Rev.* 238: 12–22.
55. Dontje, W., R. Schotte, T. Cupedo, M. Nagasawa, F. Scheeren, R. Gimeno, H. Spits, and B. Blom. 2006. Delta-like1-induced Notch1 signalling regulates the human plasmacytoid dendritic cell versus T cell lineage decision through control of GATA-3 and Spi-B. *Blood* 107: 2446–2452.